Method

Density separation of petrous bone powders for optimized ancient DNA yields

Daniel M. Fernandes,[1,2,3] Kendra A. Sirak,[4,5] Olivia Cheronet,[1,3] Mario Novak,[6] Florian Brück,[1] Evelyn Zelger,[1] Alejandro Llanos-Lizcano,[1] Anna Wagner,[1] Anna Zettl,[1] Kirsten Mandl,[1] Kellie Sara Duffet Carlson,[1,3] Victoria Oberreiter,[1,3] Kadir T. Özdoğan,[1,7] Susanna Sawyer,[1] Francesco La Pastina,[8] Emanuela Borgia,[9] Alfredo Coppa,[1,3,10] Miroslav Dobeš,[11] Petr Velemínský,[12] David Reich,[4,5] Lynne S. Bell,[13] and Ron Pinhasi[1,3]

[1]Department of Evolutionary Anthropology, University of Vienna, 1030 Vienna, Austria; [2]CIAS, Department of Life Sciences, University of Coimbra, 3000-456 Coimbra, Portugal; [3]Human Evolution and Archaeological Sciences Forschungsverbund, University of Vienna, 1030 Vienna, Austria; [4]Department of Genetics, Harvard Medical School, Boston, Massachusetts 02115, USA; [5]Department of Human Evolutionary Biology, Harvard University, Cambridge, Massachusetts 02138, USA; [6]Centre for Applied Bioanthropology, Institute for Anthropological Research, 10000 Zagreb, Croatia; [7]Department of History and Art History, Utrecht University, 3512 BS Utrecht, The Netherlands; [8]Department of Archaeology, University of Cambridge, Cambridge CB2 3DZ, United Kingdom; [9]Dipartimento di Scienze dell'Antichità, Sapienza Università di Roma, Rome 00185, Italy; [10]Dipartimento di Biologia Ambientale, Sapienza Università di Roma, Rome 00185, Italy; [11]Institute of Archaeology of the Czech Academy of Sciences, Prague 118 00, Czech Republic; [12]Department of Anthropology, National Museum, Prague 115 79, Czech Republic; [13]Centre for Forensic Research, School of Criminology, Simon Fraser University, Burnaby, British Columbia V5A 1S6, Canada

Density separation is a process routinely used to segregate minerals, organic matter, and even microplastics, from soils and sediments. Here we apply density separation to archaeological bone powders before DNA extraction to increase endogenous DNA recovery relative to a standard control extraction of the same powders. Using nontoxic heavy liquid solutions, we separated powders from the petrous bones of 10 individuals of similar archaeological preservation into eight density intervals (2.15 to 2.45 g/cm^3, in 0.05 increments). We found that the 2.30 to 2.35 g/cm^3 and 2.35 to 2.40 g/cm^3 intervals yielded up to 5.28-fold more endogenous unique DNA than the corresponding standard extraction (and up to 8.53-fold before duplicate read removal), while maintaining signals of ancient DNA authenticity and not reducing library complexity. Although small 0.05 g/cm^3 intervals may maximally optimize yields, a single separation to remove materials with a density above 2.40 g/cm^3 yielded up to 2.57-fold more endogenous DNA on average, which enables the simultaneous separation of samples that vary in preservation or in the type of material analyzed. While requiring no new ancient DNA laboratory equipment and fewer than 30 min of extra laboratory work, the implementation of density separation before DNA extraction can substantially boost endogenous DNA yields without decreasing library complexity. Although subsequent studies are required, we present theoretical and practical foundations that may prove useful when applied to other ancient DNA substrates such as teeth, other bones, and sediments.

[Supplemental material is available for this article.]

Over the past decade, there has been a concerted effort to improve the efficiency of DNA recovery from irreplaceable archaeological specimens, such as human bones and teeth. The majority of ancient DNA research is now performed using skeletal elements that have biologically higher endogenous DNA contents, such as petrous bones, ear ossicles, and tooth cementum (Gamba et al. 2014; Damgaard et al. 2015; Pinhasi et al. 2015; 2019; Hansen et al. 2017; Sirak et al. 2020; Harney et al. 2021). Ancient DNA–specific wet laboratory protocols have increased the quantity of DNA isolated and extracted (Dabney et al. 2013; Rohland et al. 2018), and improved the efficiency of DNA library construction using single-stranded molecules (Gansauge and Meyer 2013, 2019; Gansauge et al. 2020; Kapp et al. 2021). "Pretreatment" steps, such as cleaning samples with a weak sodium hypochlorite (bleach) solution (Kemp and Smith 2005), implementing a chemical or enzymatic "predigestion" step (Damgaard et al. 2015; Korlević et al. 2015; Schroeder et al. 2019), or using a combination of the two (Boessenkool et al. 2017), aim to reduce contamination and maximize endogenous DNA yields; however, these steps reduce the complexity of genomic sequencing libraries, negatively influencing downstream analyses. Here, we present a different

Corresponding authors: ron.pinhasi@univie.ac.at, daniel.fernandes@univie.ac.at
Article published online before print. Article, supplemental material, and publication date are at https://www.genome.org/cgi/doi/10.1101/gr.277714.123.

type of "pretreatment" step that improves endogenous DNA yields while not decreasing the complexity of sequencing libraries.

After the death of a vertebrate organism, the chemical composition of its skeletal remains immediately starts to be altered by diagenetic processes such as hydrolysis, enzymatic action, mineral dissolution, and microbial colonization (Bell et al. 2001; Hedges 2002; Booth 2016; Kendall et al. 2018; Rasmussen et al. 2019). These processes have substantial and irreversible effects on the structure and composition of bone, inducing collagen loss and alteration of the ratio of organic to inorganic fractions. Microorganisms, in particular, have been shown to play an important role in the mineralization of bone elements and can, therefore, cause deviations in localized density (Bell et al. 2001; Daniel and Chin 2010). As this process is one of the main pathways for the introduction of exogenous contaminant DNA, avoiding or eliminating these exogenous mineralized pockets before DNA extraction may facilitate the recovery of greater amounts of endogenous DNA.

In vivo bone naturally contains regions of differing densities. As an individual ages, new bone formation is accompanied by the progressive mineralization of existing bone matrix and osteocytes, in parallel with bone remodeling generating new osteonal systems, leading to regions of different densities within the same bone (Bell et al. 2001, 2008; Kendall et al. 2018). In petrous bones and ear ossicles, however, there is a lack of bone remodeling after ~24 wk in utero (Hernandez et al. 2004), contributing to a high concentration of mineralized osteocytes in relation to other bones (Hernandez et al. 2004; Bell et al. 2008; Ibrahim et al. 2022), and this has been hypothesized to be one of the main determinants of the success of petrous bones in the retrieval of ancient DNA (Pinhasi et al. 2019; Ibrahim et al. 2022).

Previous work has used density separation, also referred to as fractionation, to isolate elements of different densities before applying isotopic analysis to successfully reconstruct the dietary habits of archaeological individuals over the last 15 yr of their lives (Bell et al. 2001). However, to the best of our knowledge, density separation has not yet been applied to the process of recovering ancient DNA from archaeological bone powders. In theory, it could be used to not only separate endogenous bone elements of different densities, specifically including mineralized osteocytes (like in the isotopic study just mentioned) but also to separate nonendogenous clusters of mineralized microorganisms and environmental sediments that sometimes cannot be removed entirely during sample processing in an ancient DNA laboratory.

Here we present a new method for isolating the most endogenous DNA-rich fractions of petrous bone powder without additional ancient DNA laboratory equipment and using a nontoxic heavy liquid named sodium polytungstate (SPT). The main objective of this work was to identify density interval(s) that contained more endogenous DNA compared with a standard extraction of bone powder from the same individual, establishing the validity of using density separation as a technique to improve DNA recovery.

To reduce the number of external and differentiating variables that could influence our results, we restricted our analyses to petrous bones from two temperate locations in Europe (for more details on the process of sample selection, see the Methods section). According to the Allen Ancient DNA Resource, of the 8797 libraries with a clearly stated skeletal source of DNA, the petrous was used for analysis 4839 times, representing more than half of all cases (teeth were used 3161 times, representing approximately another one-third of all cases, and all other elements were used in only ~10% of cases) and is, therefore, the most likely element to which such a new methodology would be applied (https://reich.hms.harvard.edu/allen-ancient-dna-resource-aadr-downloadable-genotypes-present-day-and-ancient-dna-data; version 54.1.p1).

Results

As there are no published data or protocols for the recovery of ancient DNA from archaeological bone powder following a density separation step, we began by following a protocol similar to that presented by Bell et al. (2001), running a small preliminary experiment (for more details, see the Methods section) to achieve the protocol presented here (illustrated in Fig. 1). Any use of the terms "density" and "density intervals" in what follows refers to a measure that approximates true densities, instead of bulk densities, as the latter are calculated considering bone porosity as contributing to the units of space and have, therefore, substantially lower values than the true densities (Lee Lyman 2021).

We selected 10 petrous bones from remains excavated from two archaeological locations in temperate parts of Europe, namely, the Bronze/Iron Age sites of Praha 5–Malà Ohrada/Jinonice, respectively, in the Czech Republic (n = 4) and the Late Antiquity/Early Medieval necropolis of Castel Sozzio (Civitella D'Agliano, Viterbo), in Italy (n = 6) (Supplemental Note S1; Supplemental Table S1). We separated, from macroscopically homogeneous bone powder generated for each individual, 150 mg of powder for sequential separation over eight density intervals that were identified in our preliminary experiment as the most relevant (<2.15, 2.15–2.20, 2.20–2.25, 2.25–2.30, 2.30–2.35, 2.35–2.40, 2.40–2.45, >2.45 g/cm^3). For convenience, all intervals are from here on referred to by their highest value (e.g., interval 2.20 refers to the interval range 2.15–2.20; 2.40, to the range 2.35–2.40). We separated a further 50 mg of powder from the same homogeneous powder for standard ancient DNA extraction that followed a previously published protocol (Dabney et al. 2013) and did not include any density separation step. After sequential separation and suspension of the powder particles over the eight density intervals, each tube's liquid density was lowered and washed with Tris-EDTA (TE) buffer to repellet the suspended bone powder and remove all traces of SPT (for details, see the Methods section) (Fig. 1).

Subsequently, DNA extraction took place using the same protocol as for the standard extractions (Fig. 1). All 90 libraries (10 × 8 intervals plus 10 standard extractions) were screened using low-coverage shotgun sequencing ("Sequencing Group 1"), and the resulting sequencing data and quality metrics were assessed (Supplemental Table S1). After identifying the two best density intervals from "Sequencing Group 1" by their percentages of unique endogenous reads, we performed additional shotgun sequencing of the same libraries (also further sequencing the standard extraction libraries) in order to obtain greater amounts of data to allow for more robust comparisons ("Sequencing Group 2"). The data from the different sequencing runs were then merged (Supplemental Table S1) and, to ensure comparability and absence of bias owing to unequal sequencing yields, were randomly subsampled to equal numbers of reads within each individual, using *seqtk* (https://github.com/lh3/seqtk) (Supplemental Table S2). To statistically compare the data from the standard extractions and the best density intervals, we computed paired Wilcoxon signed-rank tests with a *P*-value threshold of significance of 0.05, a minimum of six paired observations, and the normalized, subsampled, and merged data for all metrics except for contamination estimates, as the latter should not be affected by random subsampling and

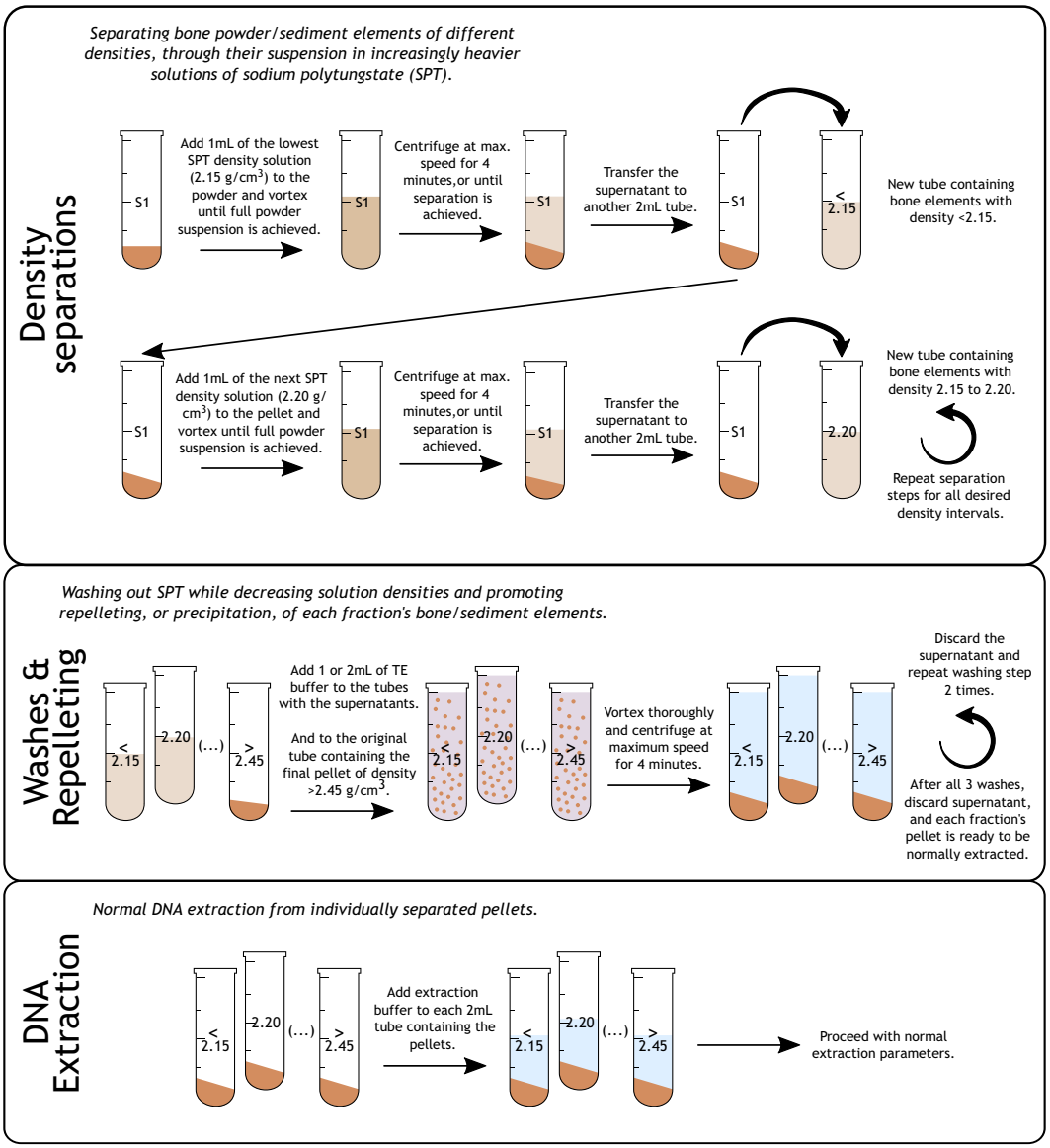

Figure 1. Diagram summarizing the three main phases of the density separation protocol for ancient DNA: sequential density separation and acquisition of the different interval solutions, washes and repelleting of the bone powders, and DNA extraction following standard methods.

benefits from more data for increased accuracy (for contamination, see Supplemental Table S1; for all other metrics, see Supplemental Table S3).

Overall, the application of the density separation protocol was successful for all individuals and densities, confirming that using SPT does not exert a negative influence on the DNA molecules or the process of DNA extraction itself. We did not weigh the exact powder amounts separated in each interval to avoid the potential introduction of contamination during the drying steps (the weight would have also been inaccurate because the powder was wet). However, a generalized sequential increase in separated repelleted powder quantities was observed along with the density, from nearly negligible amounts at <2.15 to substantial amounts at 2.40 and 2.45, with the largest pellet always present in the heaviest density interval, >2.45 g/cm^3 (Supplemental Figs. S1, S2). The assessment of the screening data across the eight density intervals indicates that the relative amounts of unique endogenous DNA (measured by the ratio of nonduplicated reads aligned to the human genome by the total number of reads) increased from 2.15 to 2.40 g/cm^3, with the highest endogenous DNA contents always present in the higher intervals: either at 2.35 or at 2.40 (Fig. 2; Supplemental Table S1). We note a single exception for individual P9884, for whom the optimal interval was 2.45 g/cm^3 (Supplemental Table S1). After resequencing and normalizing the data, these best intervals and standard extractions were compared further (Supplemental Table S2). Here, the average fraction of endogenous unique DNA reads for the standard extractions was 13.25% (range, 4.79%–26.55%), whereas for the best SPT intervals it was 32.86% (range, 20.76%–45.01%), represented by an average improvement of 3.04-fold (range, 1.53–5.28) per individual (Fig. 3A; Supplemental Table S2). The smallest change was for individual P9898, from 26.55% endogenous DNA in the standard extraction powder to

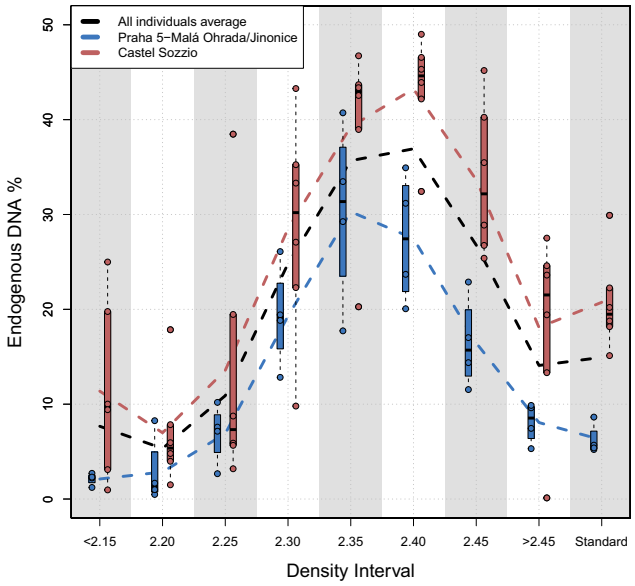

Figure 2. Distribution (bar plots) and averages (colored lines) of endogenous DNA percentages after duplicate removal, per interval and per site, using the initial sequencing data ("Sequencing Group 1") (Supplemental Table S1).

40.62% in the 2.40 g/cm^3 interval, whereas the largest was for individual 2338, from 5.41% in the standard extraction to 28.54% in the 2.35 g/cm^3 interval (Fig. 3A; Supplemental Table S2). Consequently, the endogenous contents of the standard extractions were found to be inversely correlated to the fold-increase obtained in the best SPT intervals (Fig. 4).

These paired differences in endogenous DNA yields were statistically significant (*P*-value = 0.001953) and were the result of an average increase of 3.04-fold in the number of unique aligned reads (*P*-value = 0.001953) (Fig. 3A; Supplemental Tables S2, S3). However, these changes can potentially be higher in samples with lower library saturation and fraction of duplicated reads after alignment, as we were able to achieve an 8.53-fold increase in endogenous contents for individual 2338 before the removal of duplicated reads, from 6.24% to 53.20% (Supplemental Table S2).

We estimated individual library contamination using a recently developed method that requires only 0.02× whole-genome coverage per sample (Huang and Ringbauer 2021). This method models and quantifies mismatches in haploid X Chromosomes as contamination and is therefore restricted to individuals who are molecularly sexed as male, which in our case corresponded to eight out of 10 individuals. The average contamination for all but one library above the 0.02× threshold in "Sequencing Group 1" (n = 32) was estimated to be 2.87% (range 1.37%–4.48%), which stands below the typical threshold of 5% for ancient DNA

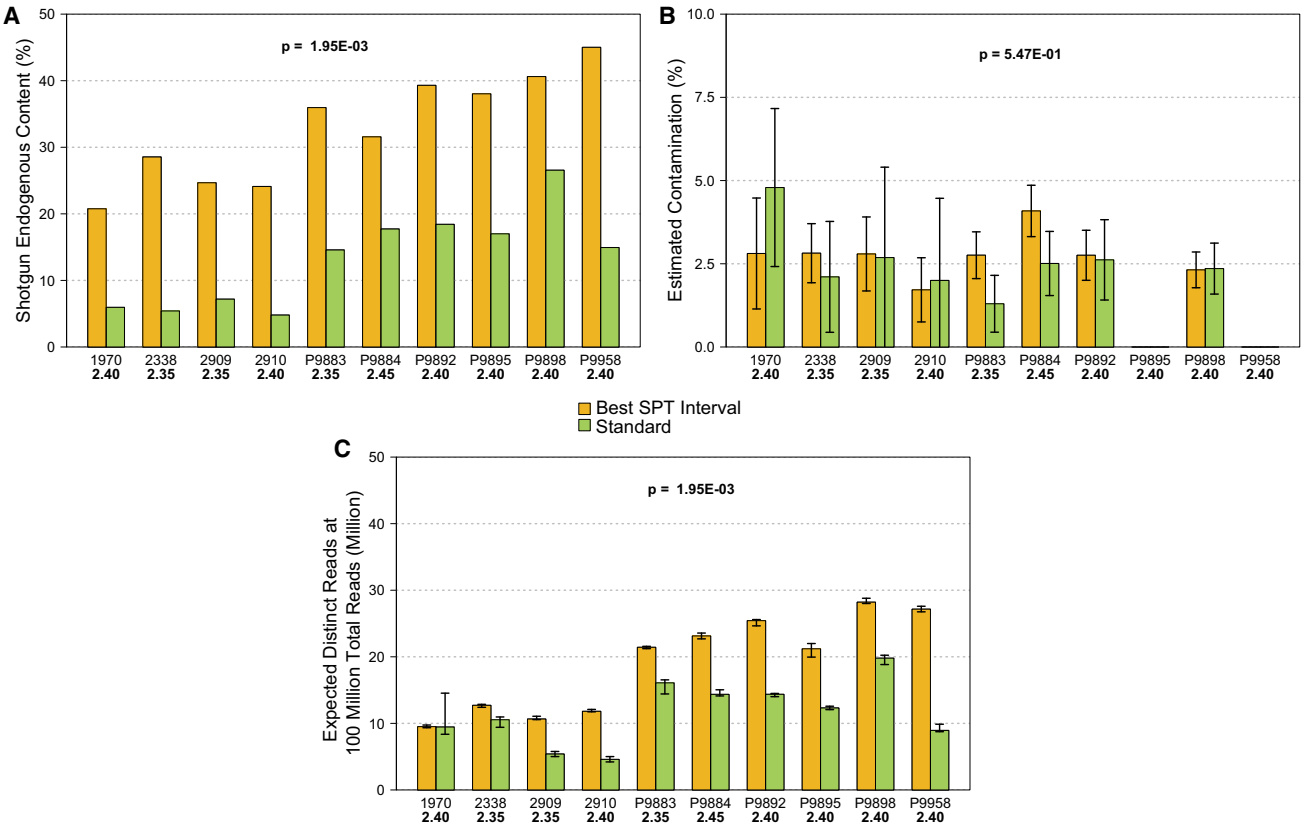

Figure 3. Comparison of some quality and authenticity metrics between the best SPT interval and the same individual's standard extraction. (*A*) Endogenous DNA contents (*P*-value = 0.001953). (*B*) Contamination estimated by hapCon for male individuals (*P*-value = 0.5469). (*C*) Expected distinct reads after deep sequencing as a measure of library complexity, estimated by *preseq* at a total number of reads of 100 million (*P*-value = 0.001953). *P*-values shown in bold denote significance under a threshold of 0.05. Panels *A* and *B* use subsampled and normalized total read numbers (Supplemental Table S2), whereas panel *C* uses the full merged data for statistical power (Supplemental Table S1).

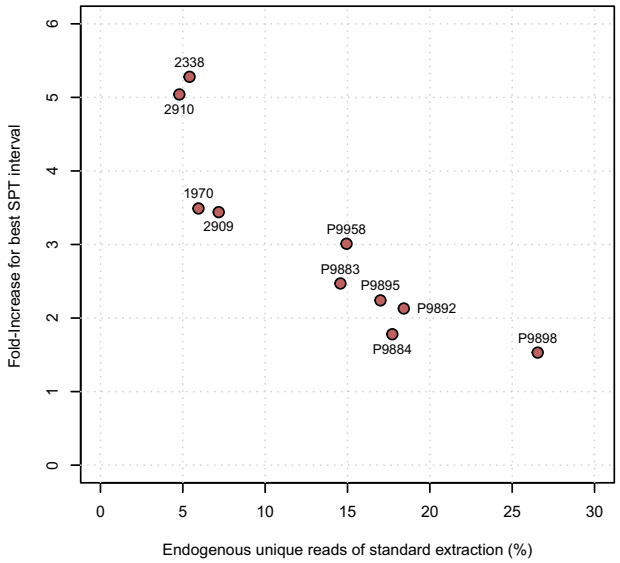

Figure 4. Fold-increase in endogenous DNA contents as a function of the standard extraction's contents. Sample IDs plotted next to each dot.

(Supplemental Table S1; Fu et al. 2013; Nakatsuka et al. 2020). One outlier had an estimated 9.9% contamination on the lower density interval (<2.15 g/cm^3 for individual P9898), which is likely an isolated observation, as the average contamination for the same individual's other six intervals and standard extraction was 2.57% (Supplemental Table S1). By then looking at the merged higher coverage data for the best intervals and the standard extraction ("Sequencing Group 2"; nonsubsampled in order to have increased analytical power), the average contamination among all was estimated to be 2.65% (range 1.30%–4.80%), with a nonsignificant difference between the best SPT intervals (average, 2.76%) and the standard extractions (average, 2.55%; *P*-value = 0.5469) (Fig. 3B; Supplemental Tables S1, S3). The negative controls included in all stages of the laboratory work support zero to negligible ancient cross-contamination, as 12/13 libraries had no terminal deamination, and the average duplication rate after polymerase chain reaction (PCR) amplification to plateau was high, at 64% (Supplemental Table S1). One control did have 0.02 terminal deamination, but only 302 sequences remained after filtering with PMDtools (threshold 3) to isolate those with the highest likelihood of being ancient (Skoglund et al. 2014).

We then investigated if separation using a wider density interval would still give better results than a standard extraction without a density separation step. A wider range that still improves DNA recovery with no introduction of contamination would enable this method to be applied simultaneously to multiple and varied samples with different preservation, taphonomic histories, and maybe even to different skeletal or other bioarchaeological DNA substrates, increasing the overall applicability of this technique. Using the screening data from "Sequencing Group 1," we found that the average endogenous DNA yields for the combined intervals 2.25, 2.30, 2.35, and 2.40 were still statistically higher than the yields of the standard extraction (*P*-value = 0.003906), with an average increase of 2.35-fold (range, 0.81–5.24) (Supplemental Tables S1, S3). To investigate this further, we used the remaining powder (between 55 and 124 mg) from the exact same batches of seven individuals after having measured the initial 150 + 50 mg, and separated them at a single density of 2.40 g/cm^3 to formally test the possibility of obtaining improved yields with a single practical separation. The average endogenous contents for the <2.40 intervals were 35.05% (range, 25.75%–47.61%), corresponding to an increase of 2.83-fold compared with the standard extractions (*P*-value = 0.01563) (Supplemental Tables S3, S4). Furthermore, for every individual, the single <2.40 interval yield was higher than the corresponding standard extraction, independently of the initial powder amount. This suggests that, although this wider density interval performed slightly worse than the narrower ones, a single separation at 2.40 g/cm^3 still provides an improvement in endogenous yields relative to a standard extraction without a preceding density separation step and that smaller initial powder amounts down to at least 50 mg can likely be used (Supplemental Tables S3, S4).

In regards to the effects of the overall increase in endogenous contents of the main set of 10 samples in other quantitative metrics, such as nuclear genomic and mitochondrial coverages, we observed an increase in both of these metrics for the best SPT intervals that was statistically significant (*P*-value = 0.001953, for both), with the average nuclear coverage increasing, on average, 2.94-fold (range, 1.58–5.04) and with the mitochondrial coverage increasing, on average, 3.12-fold (range, 1.87–5.01) (Supplemental Tables S2, S3). Similarly, when we looked at the curves produced by *preseq*'s (Daley and Smith 2013) *lc_extrap* command as a measure of library complexity, which extrapolates the expected number of distinct reads after extensive sequencing from duplication rates, we found a statistically significant average increase of 1.77-fold in the number of distinct reads at a sequencing effort of 100 million reads for the best SPT intervals (*P*-value = 0.001953) (Figs. 3C, 5; Supplemental Tables S3, S5). Although these results can be interpreted as suggesting an increase in observed library complexity, we were not able to investigate changes in complexity per milligram of input powder owing to the lack of the latter's measurements.

Lastly, the average read length of 57 bp in the standard extracts (range, 50–67 bp) was not statistically different from the average of 55 bp in the best SPT intervals (range, 51–63 bp; *P*-value = 0.1641) (Supplemental Tables S2, S3). However, we observed significant differences in deamination frequencies in the terminal bases of the DNA. These chemical alterations to the DNA in the form of C > T and G > A changes have been shown to be characteristic of ancient DNA and are one of the most important metrics for assessing authenticity (Green et al. 2009; Ginolhac et al. 2011; Sawyer et al. 2012). We observed an increase in the average deamination frequencies of the terminal bases of the 5′ end of the DNA sequences from 0.32 in the standard extracts (range, 0.27–0.40) to 0.34 in the best SPT intervals (range, 0.31–0.44), with a *P*-value of 0.003906 (Supplemental Tables S2, S3). A similar pattern was observed for the 3′ end (Supplemental Tables S2, S3). Our data do not suggest that these were caused by chemical exposure to the SPT and/or its low pH, as there was no consistent pattern between exposure to higher SPT concentrations and higher deamination. Furthermore, an expected pattern in which higher contamination would lead to lower deamination was also not observed. Nevertheless, future investigations will be able to shed more light onto this situation.

Discussion

We performed density separation of bone powder across eight sequential density intervals as an alternative type of "pretreatment" step to increase unique endogenous ancient DNA yields

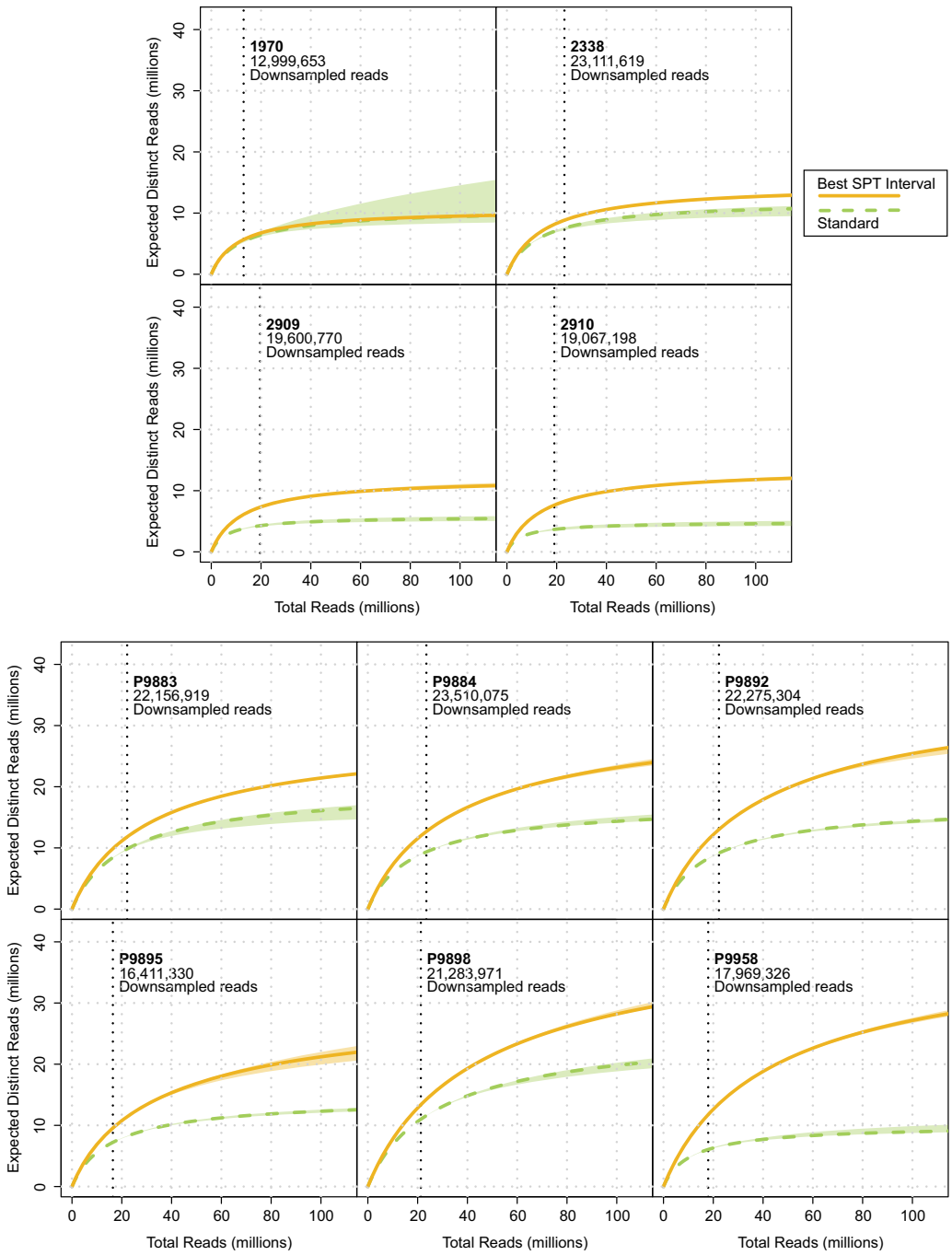

Figure 5. Yield of expected distinct reads for a theoretically larger sequencing effort, as a measure of library complexity, using the *lc_extrap* function of the software *preseq*. Vertical dotted lines represent the number of reads to which each sample's best SPT interval and standard extraction was randomly downsampled. Shaded areas represent 95% confidence intervals. Results shown here for up to 100 million total reads; in Supplemental Figure S3, for up to 500 million.

without decreasing library complexity or negatively impacting DNA authenticity. When a density separation step was implemented, we observed an up to 5.28-fold increase in unique endogenous DNA recovery, reflecting a more efficient exclusion of contaminant-rich bone elements and leading to higher ratios of endogenous DNA on normalized total read numbers. All authenticity metrics examined were similar to those for the standard extractions, and library complexity based on expected distinct reads extrapolations was never reduced for the best SPT intervals, contrary to the results observed following other pretreatment techniques such as the use of bleach to reduce surface contamination. As such, a density separation step can provide an efficient way to improve the cost efficiency of ancient DNA sequencing without requiring additional laboratory equipment.

Notably, the largest improvements in endogenous unique DNA yield were observed for the samples with the lowest yields obtained for the standard extraction. On average, we saw an increase of 4.31-fold on samples with <10% endogenous DNA yield on the standard extraction, whereas for samples with >10%, that increase was 2.19-fold, suggesting that density separation may enable the re-evaluation and analysis of previously processed samples that failed to pass the quality and quantity thresholds that rendered them inappropriate for further sequencing or population genomics analysis.

The consistency in the best density intervals identified across all samples confirms that the theoretical background of this method is valid and that, in samples with similar preservation, particles rich in endogenous DNA will be concentrated at a specific shared density range. It also confirms the validity of our selection of intervals for this experiment, as the best intervals included the higher density intervals (2.35 and 2.40) but not, except for a single sample, the interval of highest density (2.45). These results also match what is described by Bell et al. (2001) regarding the 2.30 to 2.40 g/cm^3 interval comprising interstitial bone and representing the most highly mineralized, and older, human bone elements, which is what is to be expected to be found in the cochlea owing to its lack of bone remodeling and high concentration of mineralized osteocytes containing endogenous DNA (Bell et al. 2008; Busse et al. 2010). However, and considering that different bone densities can be associated with different mineralization levels (Bell et al. 2008), variations between the various elements of the skeleton are expected, and further work should focus on the identification of each element's most optimal density intervals.

For example, as most bones are expected to have an overall lower density than the cochlea owing to constant bone remodeling, which results in a higher proportion of recently formed, lower density bone, those intervals might be slightly lower but, nevertheless, >1.7 g/cm^3 (Currey 1984; Simmons et al. 1991; Cameron et al. 1993; Bell et al. 2001; Lee Lyman 2021). In the case of (fresh) teeth, specifically, it has been shown that cementum and dentin can be separated both from enamel and each other, using individual density fractionation intervals (2.04, 2.20–2.40, and 2.70–2.80 g/cm^3, respectively) (Brekhus and Armstrong 1935). On the other hand, poorly preserved teeth and/or bones that have undergone substantial mineralization and fossilization over long time periods, may present an overall shift toward higher density intervals (Sillen 1981; Bell et al. 2001; Daniel and Chin 2010). Although no studies exist for human bones, this was shown in a gazelle bone from the Natufian period, for which the general density range moved from 1.9–2.3 g/cm^3 to 2.4–2.6 g/cm^3 (Sillen 1981; Bell et al. 2001). Thus, further studies may help us to understand if such shifts happen differentially across human bones, determine the rates at which they occur, and provide additional insight into where within the bone tissue structure the DNA is preserved (if it is still present).

Moreover, in a similar manner as to how oxygen isotopes from tooth enamel can be used to investigate individual mobility between childhood and adulthood (Budd et al. 2004; Pellegrini et al. 2016), the fact that different mineralization and density levels within the same bone are associated with differential bone formation over the last 15 yr of life of an individual (Bell et al. 2001, 2008) may prove extremely useful for future studies involving changes in ancient epigenetics and methylation patterns over a substantial period of the individual's life. Furthermore, because our proposed protocol includes several SPT wash steps, we argue that the fractions not used for ancient DNA isolation could be used in parallel for isotopic analysis. However, experimental confirmation of lack of SPT reactivity is required.

Sedimentary samples may also be a good candidate substrate for the application of density separation for ancient DNA extraction, as it may provide a way to segregate bone elements from substantially heavier and lighter soil minerals that should be richer in environmental DNA. Similarly, the same is likely also true for petrous bone powder samples obtained through cranial base drilling of complete skulls, as these often include soil particles that become loose owing to drilling vibrations and are very hard to be completely excluded from the final powder (Sirak et al. 2017).

All these possibilities create an almost endless array of follow-up investigations to the application of density separation in the field of ancient DNA and may even open up new possibilities for re-evaluating old stored powders or bones that previously did not yield workable amounts of endogenous DNA. By using a nontoxic, inexpensive, and easily accessible chemical reagent and requiring only a microcentrifuge (which is a staple equipment in any molecular DNA laboratory), density separation using SPT can be integrated into any existing ancient DNA laboratorial pipeline as a pretreatment step before DNA extraction that optimizes DNA recovery.

Methods

Selection of density intervals through preliminary experimentation

By following existing research (Simmons et al. 1991; Bell et al. 2001) and to have a more general view of the distribution of ancient DNA during the first application of SPT density separation to archaeological bone powder, we initially separated 300 mg from three ancient individuals in 0.2 g/cm^3 intervals for the range of 1.6 to 2.8 g/cm^3. Because of an imperfect first adaptation of the method to ancient bone powders, most of the tested intervals were lost during processing and were not sequenced; however, we did obtain data that showed that the intervals below 2.00 and above 2.40 g/cm^3 yielded no endogenous DNA or extremely small amounts. Instead, we found that most of the DNA was present between 2.20 and 2.40 g/cm^3. This preliminary data were in agreement with the results of the existing literature, indicating that the best density intervals for ancient human bones was between 2.00 and 2.40 g/cm^3 and, more specifically, between 2.30 and 2.40 g/cm^3 for the more mineralized bone elements (Bell et al. 2001), and formed the basis for our future work. We therefore decided to analyze the 2.20–2.40 range, and to increase specificity and accuracy, we used smaller 0.05 intervals. Given the observation that even minute amounts of bone powder were being separated, instead of the large initial amount of 300 mg of powder, we subsequently used only 150 mg. Lastly, we also included one extra interval on each side, ending up with 2.15 and 2.45 g/cm^3, plus the analysis of the elements below 2.15 and above 2.45, resulting in eight density intervals per sample plus the standard extraction in a total of 90 independent powder aliquots for DNA extraction and sequencing (<2.15, 2.20, 2.25, 2.30, 2.35, 2.40, 2,45, >2.45, standard extraction).

Sample selection and processing

Because of the varied chemical and physical composition of different skeletal elements and how they are affected by many different variables such as overall preservation, taphonomic pathways, chronological age, exposure to sudden environmental changes, and others, measured densities will vary on an individual and

elemental basis. A global and optimal density separation method for every single individual or sample type is therefore very unlikely. For this study, to reduce the number of external variables that could affect ancient DNA yields and quality and therefore inhibit our ability to detect statistically significant patterns and trends, we decided to use two sets of skeletal elements from individuals with similar preservation. The petrous bones were processed according to published protocols (Pinhasi et al. 2019) in dedicated ancient DNA facilities at the Department of Evolutionary Anthropology of the University of Vienna, where the cochleae were isolated and milled to homogeneous powder in a Retsch ball mixer mill MM 400 at maximum frequency (30 Hz) for two 30-sec sessions with a 10-sec pause between to allow for the dissipation of any heat built up. Two powder aliquots were prepared for each individual: one of 150 mg for density separation, and another of 50 mg for ancient DNA extraction using traditional protocols.

Density separation and DNA extractions

SPT (TC-Tungsten Compounds) was chosen to create heavy liquid solutions owing to its ease and safety of use for the researcher, being inorganic, nontoxic, and highly soluble in water. Furthermore, it has a large density range (~1.10 to 3.1 g/cm^3) and is thought to be inert against DNA. On the other hand, changes in its pH (2–3) affect its stability and may lead to chemical modifications and the transformation into sodium paratungstate, which is insoluble in water, and when in contact with ethanol, SPT creates a white precipitate that may have an unknown effect on, or may inhibit, PCR reactions (R. Kamps, pers. comm.). DNA library inhibition was not assessed during our experiments as this white precipitate was never observed. To ensure precision down to the 0.05 g/cm^3 intervals, we started by preparing SPT solutions for the eight specified densities by creating a calibration curve based on the 3° polynomial trend line of 15 measured densities (Supplemental Table S6). Before use, these SPT solutions were then UV irradiated for 10 min. Starting with the lowest density solution (2.15), 1 mL of it was transferred to a 2-mL Eppendorf tube containing 150 mg of bone powder, and the contents were thoroughly mixed by vortexing. After 4 min of centrifugation at maximum speed (20,238*g*), all powder elements heavier than the density used (here, 2.15 g/cm^3) sank into a pellet, whereas the supernatant contained a suspension of elements ≤2.15 g/cm^3. The supernatant was transferred into a new 2-mL tube and labeled according to its density interval: here, <2.15 (Fig. 1). Although not specifically required, wide-bore tips can be useful for this step. Then, 1 mL of the next density, 2.20, was transferred into the tube with the pellet, and the process was repeated. In this case, elements lighter than 2.20 (and heavier than the previous density, 2.15) remained in suspension, whereas the heavier elements, again, formed the pellet that was used for the next density separation. This process was then repeated for all densities. The last tube obtained using the SPT solution of 2.45 g/cm^3 contained a pellet with elements heavier than 2.45 and a supernatant with elements between 2.40 and 2.45. As mentioned above, both were further processed, extracted, and sequenced.

After all separations were achieved, each tube with the newly separated elements suspended in 1 mL of SPT went through a wash and repelleting phase by adding 1 mL of TE buffer to each tube in order to lower the liquid solution's density and force the pelleting of the now-heavier bone elements. The addition of 1 mL of TE buffer lowers the density of the SPT solutions to between 1.67 and 1.73 g/cm^3, for the 2.15 and the 2.40 tubes, respectively, which should be lower than any existing bone elements and, therefore, should force them to repellet. After vortexing, each tube was centrifuged at maximum speed for 4 min, and the supernatant containing low-density SPT + TE was discarded. To ensure a thorough removal of the SPT, this wash/repelleting step was repeated two times. Although not requiring repelleting, the >2.45 tube with the final pellet was also washed three times to remove all SPT traces. If this, or any other pellet, is somewhat large (e.g., >50–100 mg), using 2 mL of TE buffer per wash is suggested.

After the washes, all pellets were ready for standard DNA extraction, which was performed using the Dabney protocol (Dabney et al. 2013), as modified by Korlević and colleagues (2015), using preassembled high pure viral nucleic acid large-volume kit spin columns from Roche instead of a custom MinElute column apparatus.

Library preparation, quality control, and sequencing

Double-stranded DNA libraries were prepared according to a modified Meyer and Kircher (2010) protocol. Individual libraries were prepared from 12.5 µL extract each, and intermediate clean-up steps were performed using Qiagen MinElute PCR purification kits to retain very short fragments (~30–80 bp). Before amplification, real-time qPCR of a small quantity of library (1 µL) was performed to assess the number of molecules present and choose the required number of cycles for amplification. All libraries were then double-indexed and amplified using Agilent PfuTurbo C_x Hotstart DNA polymerase. Before sequencing, libraries were quantified using Qubit and TapeStation or Bioanalyzer. The libraries, plus negative controls for each laboratorial step, were then sequenced on an Illumina NovaSeq SP SR100 XP at the Vienna BioCenter Core Facilities.

Data processing

Raw sequencing data were processed with cutadapt (v2.3) (Martin 2011) to remove library adapters and barcodes from the DNA sequences, allowing for 1-bp overlap and excluding sequences <18 bp. These sequences were then aligned to the human reference genome hg19, with the mitochondrial genome replaced by the RCRS sequence, using BWA's (v0.7.17-r1188) (Li and Durbin 2009) *aln* command with seeding disabled using -l 1000. We note that the great majority of published ancient DNA data has been aligned to the human genome reference hg19, and therefore, we did the same for consistency. Moreover, an alignment to GRCh38 would not be expected to alter our findings, as our results are based on quantitative comparisons of sample metrics, rather than on population genomic analyses. The alignments were then converted to the SAM format using BWA's *samse* command and, subsequently, again converted to BAM format with SAMtools *view* (v1.1) (Li et al. 2009) using the quality filter -q 30 and discarding unmapped sequences with -F 4. Duplicated sequences were removed using SAMtools' *rmdup* command. Terminal deamination was assessed using mapDamage (v2.0) (Jónsson et al. 2013); contamination was assessed on the haploid X Chromosome of males using hapCon with a threshold of 0.02× or 2000 SNPs (Huang and Ringbauer 2021); and molecular sex was determined by looking at the fraction of sequences aligning to the Y Chromosome compared with the total fraction aligning to both sex chromosomes (Skoglund et al. 2013). To randomly subsample FASTQ files for reanalysis of merged libraries, *seqtk* (https://github.com/lh3/seqtk) was used. Library complexity curves were estimated using the *lc_extrap* command from *preseq* (v2.0.2) on the merged down-sampled BAM files before duplicate removal, with default settings (Daley and Smith 2013). Statistical significance tests were performed in R (v4.2.1) using the function wilcox.test(), as well as wilcox.exact() when ties were present, and the argument paired=TRUE (R Core Team 2022).

Data access

The raw sequencing data generated in this study have been submitted to the European Nucleotide Archive (ENA; https://www.ebi.ac.uk/ena/browser/) under accession number PRJEB60553.

Competing interest statement

The authors declare no competing interests.

Acknowledgments

We thank Michael Hofreiter and Nadin Rohland for their input and helpful discussions. Funding was provided by the University of Vienna Research Platform: Mineralogical Preservation of the Human Biome from the Depth of Time (MINERVA). S.S. was funded by the Austrian Science Fund (FWF) M3108-G. This work was also partially supported by a Young Investigator Award to D.M.F. from the Faculty of Life Sciences of the University of Vienna. The excavation of Castel Sozzio was funded by the Grandi Scavi program of the Sapienza University of Rome.

References

Bell LS, Cox G, Sealy J. 2001. Determining isotopic life history trajectories using bone density fractionation and stable isotope measurements: a new approach. *Am J Phys Anthropol* **116:** 66–79. doi:10.1002/ajpa.1103

Bell LS, Kayser M, Jones C. 2008. The mineralized osteocyte: a living fossil. *Am J Phys Anthropol* **137:** 449–456. doi:10.1002/ajpa.20886

Boessenkool S, Hanghøj K, Nistelberger HM, Der Sarkissian C, Gondek AT, Orlando L, Barrett JH, Star B. 2017. Combining bleach and mild predigestion improves ancient DNA recovery from bones. *Mol Ecol Resour* **17:** 742–751. doi:10.1111/1755-0998.12623

Booth TJ. 2016. An investigation into the relationship between funerary treatment and bacterial bioerosion in European archaeological human bone. *Archaeometry* **58:** 484–499. doi:10.1111/arcm.12190

Brekhus PJ, Armstrong WD. 1935. A method for the separation of enamel, dentin, and cementum. *J Dent Res* **15:** 23–29. doi:10.1177/00220345350150010401

Budd P, Millard A, Chenery C, Lucy S, Roberts C. 2004. Investigating population movement by stable isotope analysis: a report from Britain. *Antiquity* **78:** 127–141. doi:10.1017/S0003598X0009298X

Busse B, Djonic D, Milovanovic P, Hahn M, Püschel K, Ritchie RO, Djuric M, Amling M. 2010. Decrease in the osteocyte lacunar density accompanied by hypermineralized lacunar occlusion reveals failure and delay of remodeling in aged human bone. *Aging Cell* **9:** 1065–1075. doi:10.1111/j.1474-9726.2010.00633.x

Cameron JR, Skofronick JG, Grant RM, Siegel E. 1993. Medical physics: physics of the body. *Am J Phys* **61:** 1156–1156. doi:10.1119/1.17319

Currey JD. 1984. *The mechanical adaptations of bones*. Princeton University Press, Princeton, NJ.

Dabney J, Knapp M, Glocke I, Gansauge M-T, Weihmann A, Nickel B, Valdiosera C, García N, Pääbo S, Arsuaga J-L, et al. 2013. Complete mitochondrial genome sequence of a Middle Pleistocene cave bear reconstructed from ultrashort DNA fragments. *Proc Natl Acad Sci* **110:** 15758–15763. doi:10.1073/pnas.1314445110

Daley T, Smith AD. 2013. Predicting the molecular complexity of sequencing libraries. *Nat Methods* **10:** 325–327. doi:10.1038/nmeth.2375

Damgaard PB, Margaryan A, Schroeder H, Orlando L, Willerslev E, Allentoft ME. 2015. Improving access to endogenous DNA in ancient bones and teeth. *Sci Rep* **5:** 11184. doi:10.1038/srep11184

Daniel JC, Chin K. 2010. The role of bacterially mediated precipitation in the permineralization of bone. *Palaios* **25:** 507–516. doi:10.2110/palo.2009.p09-120r

Fu Q, Meyer M, Gao X, Stenzel U, Burbano HA, Kelso J, Pääbo S. 2013. DNA analysis of an early modern human from Tianyuan Cave, China. *Proc Natl Acad Sci* **110:** 2223–2227. doi:10.1073/pnas.1221359110

Gamba C, Jones ER, Teasdale MD, McLaughlin RL, Gonzalez-Fortes G, Mattiangeli V, Domboróczki L, Kővári I, Pap I, Anders A, et al. 2014. Genome flux and stasis in a five millennium transect of European prehistory. *Nat Commun* **5:** 5257. doi:10.1038/ncomms6257

Gansauge M-T, Meyer M. 2013. Single-stranded DNA library preparation for the sequencing of ancient or damaged DNA. *Nat Protoc* **8:** 737–748. doi:10.1038/nprot.2013.038

Gansauge M-T, Meyer M. 2019. A method for single-stranded ancient DNA library preparation. *Methods Mol Biol* **1963:** 75–83. doi:10.1007/978-1-4939-9176-1_9

Gansauge M-T, Aximu-Petri A, Nagel S, Meyer M. 2020. Manual and automated preparation of single-stranded DNA libraries for the sequencing of DNA from ancient biological remains and other sources of highly degraded DNA. *Nat Protoc* **15:** 2279–2300. doi:10.1038/s41596-020-0338-0

Ginolhac A, Rasmussen M, Gilbert MTP, Willerslev E, Orlando L. 2011. mapDamage: testing for damage patterns in ancient DNA sequences. *Bioinformatics* **27:** 2153–2155. doi:10.1093/bioinformatics/btr347

Green RE, Briggs AW, Krause J, Prüfer K, Burbano HA, Siebauer M, Lachmann M, Pääbo S. 2009. The Neandertal genome and ancient DNA authenticity. *EMBO J* **28:** 2494–2502. doi:10.1038/emboj.2009.222

Hansen HB, Damgaard PB, Margaryan A, Stenderup J, Lynnerup N, Willerslev E, Allentoft ME. 2017. Comparing ancient DNA preservation in petrous bone and tooth cementum. *PLoS One* **12:** e0170940. doi:10.1371/journal.pone.0170940

Harney É, Cheronet O, Fernandes DM, Sirak K, Mah M, Bernardos R, Adamski N, Broomandkhoshbacht N, Callan K, Lawson AM, et al. 2021. A minimally destructive protocol for DNA extraction from ancient teeth. *Genome Res* **31:** 472–483. doi:10.1101/gr.267534.120

Hedges REM. 2002. Bone diagenesis: an overview of processes. *Archaeometry* **44:** 319–328. doi:10.1111/1475-4754.00064

Hernandez CJ, Majeska RJ, Schaffler MB. 2004. Osteocyte density in woven bone. *Bone* **35:** 1095–1099. doi:10.1016/j.bone.2004.07.002

Huang Y, Ringbauer H. 2021. hapCon: estimating contamination of ancient genomes by copying from reference haplotypes. *Bioinformatics* **38:** 3768–3777. doi:10.1093/bioinformatics/btac390

Ibrahim J, Brumfeld V, Addadi Y, Rubin S, Weiner S, Boaretto E. 2022. The petrous bone contains high concentrations of osteocytes: one possible reason why ancient DNA is better preserved in this bone. *PLoS One* **17:** e0269348. doi:10.1371/journal.pone.0269348

Jónsson H, Ginolhac A, Schubert M, Johnson PLF, Orlando L. 2013. mapDamage2.0: fast approximate Bayesian estimates of ancient DNA damage parameters. *Bioinformatics* **29:** 1682–1684. doi:10.1093/bioinformatics/btt193

Kapp JD, Green RE, Shapiro B. 2021. A fast and efficient single-stranded genomic library preparation method optimized for ancient DNA. *J Hered* **112:** 241–249. doi:10.1093/jhered/esab012

Kemp BM, Smith DG. 2005. Use of bleach to eliminate contaminating DNA from the surface of bones and teeth. *Forensic Sci Int* **154:** 53–61. doi:10.1016/j.forsciint.2004.11.017

Kendall C, Eriksen AMH, Kontopoulos I, Collins MJ, Turner-Walker G. 2018. Diagenesis of archaeological bone and tooth. *Palaeogeogr Palaeoclimatol Palaeoecol* **491:** 21–37. doi:10.1016/j.palaeo.2017.11.041

Korlević P, Gerber T, Gansauge M-T, Hajdinjak M, Nagel S, Aximu-Petri A, Meyer M. 2015. Reducing microbial and human contamination in DNA extractions from ancient bones and teeth. *BioTechniques* **59:** 87–93. doi:10.2144/000114320

Lee Lyman R. 2021. Bone density and bone attrition. In *Manual of forensic taphonomy* (ed. Pokines JT, et al.), pp. 79–102. CRC Press, Boca Raton, FL.

Li H, Durbin R. 2009. Fast and accurate short read alignment with Burrows–Wheeler transform. *Bioinformatics* **25:** 1754–1760. doi:10.1093/bioinformatics/btp324

Li H, Handsaker B, Wysoker A, Fennell T, Ruan J, Homer N, Marth G, Abecasis G, Durbin R, 1000 Genome Project Data Processing Subgroup. 2009. The Sequence Alignment/Map format and SAMtools. *Bioinformatics* **25:** 2078–2079. doi:10.1093/bioinformatics/btp352

Martin M. 2011. Cutadapt removes adapter sequences from high-throughput sequencing reads. *EMBnet.J* **17:** 10. doi:10.14806/ej.17.1.200

Meyer M, Kircher M. 2010. Illumina sequencing library preparation for highly multiplexed target capture and sequencing. *Cold Spring Harb Protoc* **2010:** pdb.prot5448. doi:10.1101/pdb.prot5448

Nakatsuka N, Harney É, Mallick S, Mah M, Patterson N, Reich D. 2020. ContamLD: estimation of ancient nuclear DNA contamination using breakdown of linkage disequilibrium. *Genome Biol* **21:** 199. doi:10.1186/s13059-020-02111-2

Pellegrini M, Pouncett J, Jay M, Pearson MP, Richards MP. 2016. Tooth enamel oxygen "isoscapes" show a high degree of human mobility in prehistoric Britain. *Sci Rep* **6:** 34986. doi:10.1038/srep34986

Pinhasi R, Fernandes D, Sirak K, Novak M, Connell S, Alpaslan-Roodenberg S, Gerritsen F, Moiseyev V, Gromov A, Raczky P, et al. 2015. Optimal ancient DNA yields from the inner ear part of the human petrous bone. *PLoS One* **10:** e0129102. doi:10.1371/journal.pone.0129102

Pinhasi R, Fernandes DM, Sirak K, Cheronet O. 2019. Isolating the human cochlea to generate bone powder for ancient DNA analysis. *Nat Protoc* **14:** 1194–1205. doi:10.1038/s41596-019-0137-7

Rasmussen KL, Milner G, Skytte L, Lynnerup N, Thomsen JL, Boldsen JL. 2019. Mapping diagenesis in archaeological human bones. *Heritage Science* **7:** 41. doi:10.1186/s40494-019-0285-7

R Core Team. 2022. *R: a language and environment for statistical computing*. R Foundation for Statistical Computing, Vienna. https://www.R-project.org/.

Rohland N, Glocke I, Aximu-Petri A, Meyer M. 2018. Extraction of highly degraded DNA from ancient bones, teeth and sediments for high-throughput sequencing. *Nat Protoc* **13:** 2447–2461. doi:10.1038/s41596-018-0050-5

Sawyer S, Krause J, Guschanski K, Savolainen V, Pääbo S. 2012. Temporal patterns of nucleotide misincorporations and DNA fragmentation in ancient DNA. *PLoS One* **7:** e34131. doi:10.1371/journal.pone.0034131

Schroeder H, de Barros Damgaard P, Allentoft ME. 2019. Pretreatment: improving endogenous ancient DNA yields using a simple enzymatic predigestion step. *Methods Mol Biol* **1963:** 21–24. doi:10.1007/978-1-4939-9176-1_3

Sillen A. 1981. Post-depositional changes in Natufian and Aurignacian faunal bones from Hayonim Cave. *Paléorient* **7:** 81–85. doi:10.3406/paleo.1981.4300

Simmons ED Jr, Pritzker KP, Grynpas MD. 1991. Age-related changes in the human femoral cortex. *J Orthop Res* **9:** 155–167. doi:10.1002/jor.1100090202

Sirak KA, Fernandes DM, Cheronet O, Novak M, Gamarra B, Balassa T, Bernert Z, Cséki A, Dani J, Gallina JZ, et al. 2017. A minimally-invasive method for sampling human petrous bones from the cranial base for ancient DNA analysis. *BioTechniques* **62:** 283–289. doi:10.2144/000114558

Sirak K, Fernandes D, Cheronet O, Harney E, Mah M, Mallick S, Rohland N, Adamski N, Broomandkhoshbacht N, Callan K, et al. 2020. Human auditory ossicles as an alternative optimal source of ancient DNA. *Genome Res* **30:** 427–436. doi:10.1101/gr.260141.119

Skoglund P, Storå J, Götherström A, Jakobsson M. 2013. Accurate sex identification of ancient human remains using DNA shotgun sequencing. *J Archaeol Sci* **40:** 4477–4482. doi:10.1016/j.jas.2013.07.004

Skoglund P, Northoff BH, Shunkov MV, Derevianko AP, Pääbo S, Krause J, Jakobsson M. 2014. Separating endogenous ancient DNA from modern day contamination in a Siberian Neandertal. *Proc Natl Acad Sci* **111:** 2229–2234. doi:10.1073/pnas.1318934111

Received January 18, 2023; accepted in revised form April 11, 2023.

Density separation of petrous bone powders for optimized ancient DNA yields

Daniel M. Fernandes, Kendra A. Sirak, Olivia Cheronet, et al.

Genome Res. published online April 18, 2023
Access the most recent version at doi:10.1101/gr.277714.123

Supplementary Material

Density separation of petrous bone powders for optimised ancient DNA yields

Fernandes et al.

Table of Contents:

Supplementary Note 1
Archaeological site descriptions

Prague 5 – Jinonice district, Holman's Garden Centre site
Prague, Central Bohemia, Czech Republic
This flat La Tène culture cemetery was discovered in the area of the former Holman's Garden Centre in Prague. The site was uncovered by archaeological rescue excavations associated with the construction of the Prague metro in the 1980s (1984-1986; City of Prague Museum). In addition to the La Tène graves, this polycultural site also yielded graves from the Neolithic, the Eneolithic and Early Bronze Age (Únětice culture).

A total of about 55 La Tène graves containing the skeletal remains of 65 individuals were discovered. The preservation of the skeletal remains was generally poor, although the site was not excavated completely. Thirty-seven individuals were included in the analyses.
Only the anthropological analyses of the excavated skeletal remains have been completely published thus far (Velemínský and Dobisíková 1998). The complex archaeological and scientific evaluation will be summarised in a monograph that is currently in preparation (Sankot 2022). The site has been dated to the 4th-3rd centuries BC on the basis of archaeological artefacts, more precisely to the LT B1b to LT C1b phases. Usually, inhumation burials are in a supine position, most often with the head towards the NNE, N or NE. A genetic profile has been carried out on some individuals from the burial site, including grave 18 (Patterson et al. 2022).

- *Grave 18*. Skeleton: inhumation burial, supine, head towards the north–east. Sex: anthropology – M, DNA – M. Age: adult, 30-50. Grave goods: iron fibula. Archaeological dating: La Tène culture. Radiocarbon dating: not available. NM Prague, Inv. No.: P7A 16113. (Sankot 2022; Velemínský and Dobisíková 1998; Patterson et al. 2022, Master_ID I16269).
- *Grave 27*. Skeleton: inhumation burial, supine, left hand on the pelvis, head towards the north–east. Sex: anthropology – ? (M?), DNA – M. Age: adult, 30–50. Grave goods: iron arm arm-ring, bronze bracelet. Archaeological dating: La Tène culture. Radiocarbon dating: not available. NM Prague, Inv. No.: P7A 16119. (Sankot 2022; Velemínský and Dobisíková 1998).
- *Grave 35*. Skeleton: inhumation burial in a slightly crouched position on the supine, left hand points, going to the pelvis, head towards the north–west. Sex: anthropology – ?, DNA – M. Age: adolescent, 12–18. Grave goods: iron bracelet fragments. Archaeological dating: La Tène culture. Radiocarbon dating: not available. NM Prague, Inv. No.: P7A 16122. (Sankot 2022; Velemínský and Dobisíková 1998).

Prague 5 – Malá Ohrada
Stodůlky area, Central Bohemia, Czech Republic
Rescue excavation due to the construction of the "Lužiny" prefab housing estate (J. Kovářík) in 1979–1980. On an area of ca 1.5 ha more than 500 settlement features (Funnel Beaker culture, Late and Final Bronze Age, Hallstatt period, Roman Iron Age) and burials (Jordanów culture – one grave, Petriščáková et al. 2016; Corded Ware culture – four graves, Buchvaldek and Kovářík 1993; Bell Beaker culture – one grave, Olalde et al. 2018; Únětice culture; Early Middle Ages) were excavated. One Corded Ware grave (Nr. 10) and 18 burials from 17 Únětice culture graves were analysed for aDNA, including grave 25 (Patterson et al 2022). The Únětice culture finds have not yet been published in detail and are only mentioned elsewhere (Smejtek 2005, 451); a monograph is being prepared (K. Petriščáková).

- *Grave 25*. Skeleton: unknown position (documentation missing). Sex: anthropology - ? (M?), DNA - M. Age: adult, 30-50. Grave goods: without finds. Archaeological dating: Únětice culture. Radiocarbon dating: not available. (Petriščáková 2011, 68-69, fig. 16; Patterson et al. 2022, Master_ID 16110). NM Prague, Inv. No.: P7A 38770. (Petriščáková 2011, 68-69, fig. 16; Patterson et al. 2022, Master_ID I16110).

Necropolis of Castel Sozzio
Municipality of Civitella D'Agliano, Viterbo, Italy

The Necropolis of Castel Sozzio is located in the Middle Tiber Valley, approximately 80 km in a straight line north of Rome, on the slopes of the hills looking at the river on its western side. This region was very important, at least since the Roman period, when it was exploited for agricultural purposes. In the Late Roman and Early Medieval periods, the situation changed and this area became a strategic border in the struggles between the Byzantines and the Goths, and, then, the Lombards.

The excavation of the necropolis was resumed in 2020 under the direction of Emanuela Borgia (Dipartimento di Scienze dell'Antichità, Sapienza Università di Roma) with an official Excavation Concession by the Soprintendenza Archeologia, Belle Arti e Paesaggio per l'Area Metropolitana di Roma, la Provincia di Viterbo e l'Etruria Meridionale, now Soprintendenza Archeologia, Belle Arti e Paesaggio per la Provincia di Viterbo e l'Etruria Meridionale (Borgia 2021).

The necropolis was connected to a rural settlement that grew up upon a Roman *villa* or *vicus*. This settlement was probably located to the east of the funerary area, but its remains are still to be investigated. At the present time, a total of 56 tombs were investigated. The burials are carved in lines in the local travertine bedrock or in the clay deposits, and pertain to different typologies: chest tombs made with, and covered by stone slabs, *cappuccina* graves, and pit graves. The tombs are mainly oriented west-east, with the head of the deceased looking east; only a few of them are oriented north-south and in this case, the deceased usually looks south. We can recognize at least four overlapping phases of tombs, pertaining to different periods of use of the funerary area. A large part of the graves was reused various times (as multiple burials reveal), often respecting the previous burials, whose bones could be moved to a sort of "ossuary-pit" near the tomb or reorganised within the tomb itself. The reuse of tombs was a highly complex procedure that forced the (maybe different) communities using the cemetery into negotiating and formalising, or even ritualizing, the way in which bodies were acted on.

All this information proves the protracted use of the necropolis in terms of time, even if the chronology of the single tombs and of their different phases of use is difficult to establish, due the almost total lack of grave goods. A preliminary interpretation based on stratigraphic data, on the few elements of furniture, and on the large reuse of *spolia* from a Roman villa in the tombs suggests a date between the late 5th-early 6th and the 7th century AD.
The tombs from which the analysed samples were taken are chiefly chest graves (tomb 7, tomb 15, tomb 16, tomb 19), whereas tomb 27 and tomb 32 are pit graves. They contained both single and multiple burials.

- *Tomb 7*, oriented west-east, contained two superimposed depositions, the uppermost of which (individual n. 1, US 175) is analysed in this work.
- *Tomb 15* is oriented west-east, and appears to be as one of the most recent in the necropolis due to stratigraphic reasons. It revealed a very complex burial situation, as it contained one primary deposition (US 210) and 8 skulls well-orderly arranged around it (US 207); one of the latter is analysed in this work (skull 5).
- *Tomb 16* is oriented north-south, and contained a single individual (US 208). It is as recent as tomb 15.

- *Tomb 13/19A* is oriented west-east, and encompassed two burials, one of which in primary deposition that is analysed here (US 162).
- *Tomb 27 and Tomb 32* are pit graves (the former deposition is numbered US 193). The latter is the most recent among those analysed here, because it was carved over an earlier chest tomb. It encompassed one single individual (US 321).

Supplementary Note 2
Supplementary References

Borgia E. 2021. La necropoli di Castel Sozzio, Civitella D'Agliano (Viterbo): note preliminari'. In *Una Terra di Mezzo. I Longobardi e la nascita della Toscana* (ed. C Valdambrini), pp. 415-419. Silvana Editoriale, Cinisello Balsamo.

Buchvaldek M. and Kovářík J. 1993. Pohřebiště se šňůrovou keramikou v Praze-Jinonicích. Doplněk ke Katalogu šňůrové keramiky v Čechách VI – Die schnurkeramischen Gräberfelder in Prag-Jinonice. Eine Ergänzung zum Katalog der Schnurkeramik in Böhmen VI. *Praehistorica* **20**: 119–174.

Olalde I, Brace S, Allentoft ME, Armit I, Kristiansen K, Booth T, Rohland N, Mallick S, Szécsényi-Nagy A, Mittnik A, et al. 2018. The Beaker phenomenon and the genomic transformation of northwest Europe. *Nature* **555**: 190–196.

Patterson N, Isakov M, Booth T, Büster L, Fischer C-E, Olalde I, Ringbauer H, Akbari A, Cheronet O, Bleasdale M, et al. 2022. Large-scale migration into Britain during the Middle to Late Bronze Age. *Nature* **601**: 588–594.

Petriščáková K. 2011. Pohrebiská v Jinoniciach, Butoviciach a Stodůlkach a regionálne špecifiká únětickej kultúry – Burial grounds at Jinonice, Butovice and Stodůlky (Prague) and regional specifics of the Únětice Culture. *Unpublished masters (diploma) dissertation*. Faculty of Arts, Charles University (FFUK), Praha.

Petriščáková K, Dobeš M, Popelka M. 2016. Neolitické a časně eneolitické hroby z Prahy – Jihozápadního Města – Late Neolithic and Early Eneolithic Graves from Prague – Jihozápadní město ...tenkrát na východě... Sborník k 80. narozeninám Víta Vokolka*. Praehistorica* **33**: 335–349.

Sankot P. 2022. Laténská pohřebiště v Praze-Ruzyni a v Praze-Jinonicích. *Archaeologica Pragensia – Supplementum 6*. The City of Prague Museum, Praha.

Smejtek L. 2005. Praha bronzová. Starší a střední doba bronzová (2200 až 1400/1300 před Kristem). In *Pravěká Praha* (ed. Lutovský M and Smejtek L. a kolecktiv), pp. 361–470. Libri, Praha.

Velemínský P. and Dobisíková M. 1998. Demografie a základní antropologická charakteristika pravěkých pohřebišť v Praze 5 – Jinonicích (Eneolit, kultura únětická, laténské období) – Demographie und die Grundlagen der anthropologischen Charakteristik der urgeschichtlichen Gräberfelder in Prag 5 – Jinonice. *Archaeologica Pragensia* **14:** 229–271.

Supplementary Figure S1

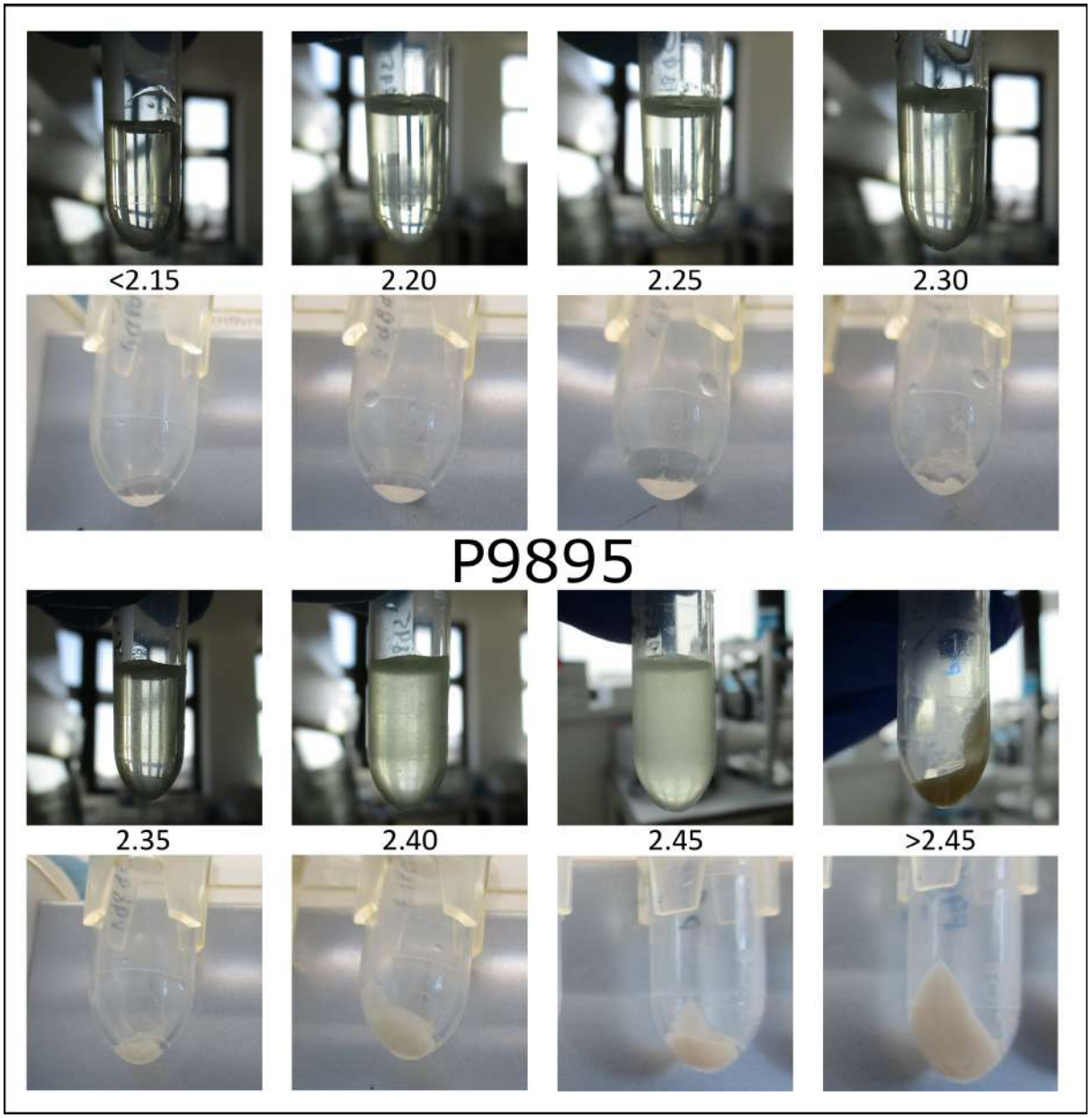

Supplementary Figure S1. Bone powder of P9895 suspended in SPT solution (top rows) and after re-pelleting and TE washes (bottom rows), for each separated interval, demonstrating increasing suspension turbidity and pellet sizes.

Supplementary Figure S2

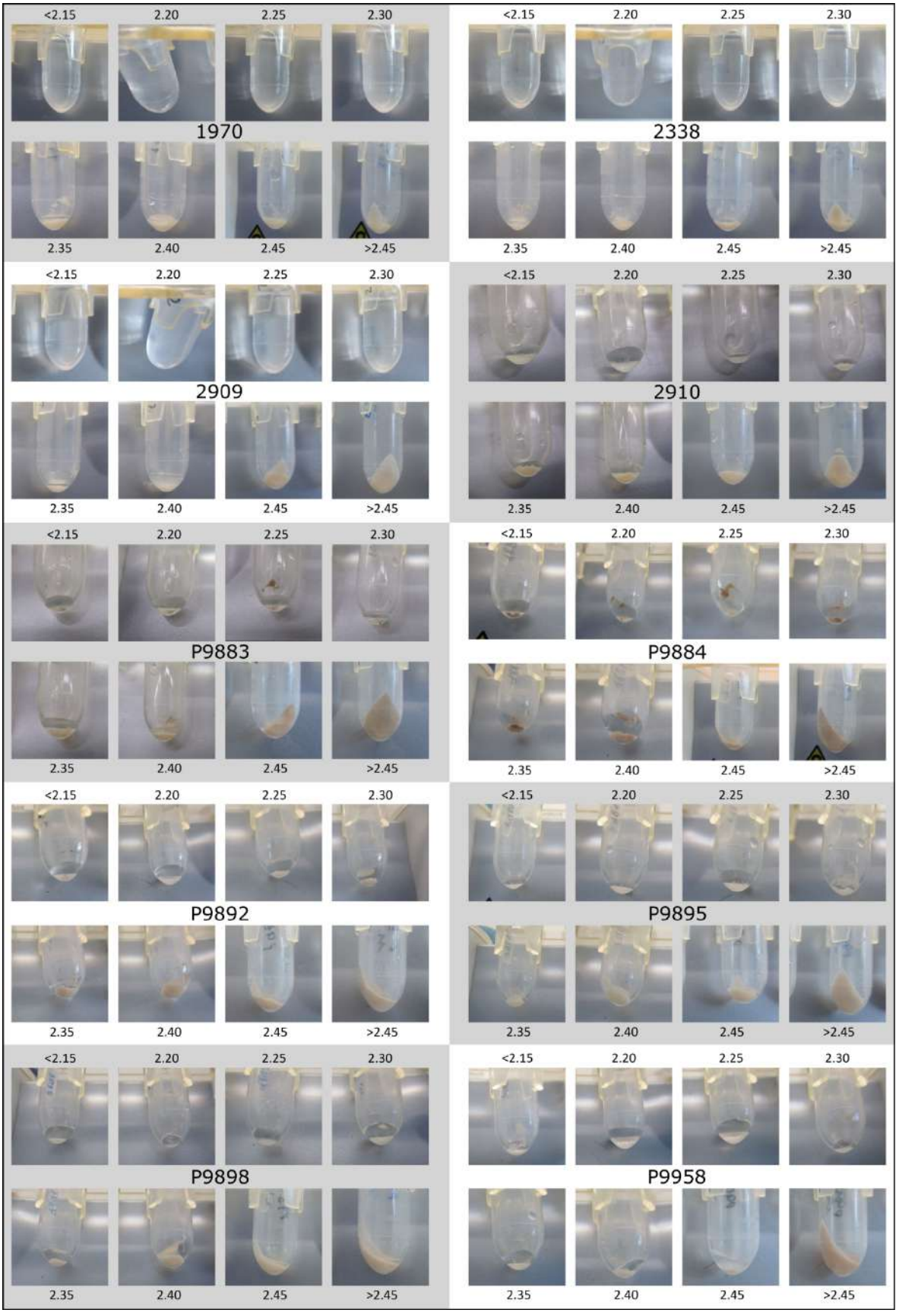

Supplementary Figure S2: Bone powder powder of all samples after re-pelleting and TE washes, for each separated interval, demonstrating increasing pellet sizes.

Supplementary Figure S3

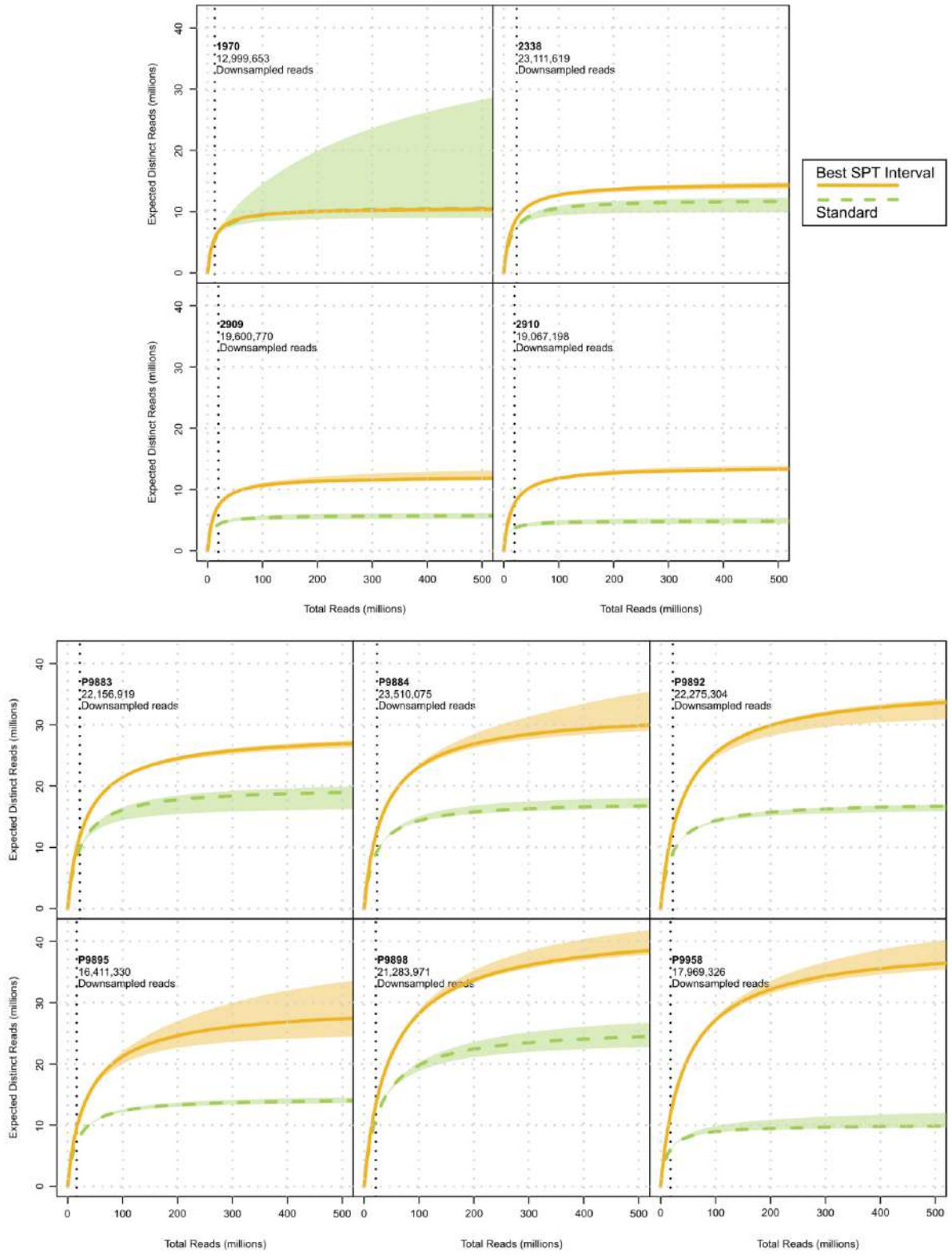

Supplementary Figure S3. Library complexity curves, based on the yield of expected distinct reads for a theoretically larger sequencing effort, using the *lc_extrap* function of the software *preseq*. Vertical dotted lines represent the number of reads each sample's best SPT interval and standard extraction were randomly downsampled to. Shaded areas represent 95% confidence intervals. Results shown here for up to 500 million total reads, and in **Figure 5** for up to 100 million.

Supplementary Table S1: Summary results and authenticity metrics for each individual sequenced library, and for the merged 2 best SPT intervals and s

Sample ID	Site	Archaeological ID	Archaeological Period	Density Interval	Sequencing ID	Sequencing Group (1=initial sequencing data; 2=extra sequencing of 2 best intervals and standard)	Total reads	Trimmed reads -O 1, -m 18
1970	Praha 5 - Jinonice, Czech Republic	Jinonice gr. 18, P7A-16113	Iron Age	Below 2.15	194591	1	5.532.636	3.921.331
				2,2	194592	1	6.994.954	5.677.764
				2,25	194593	1	7.717.018	5.823.617
				2,3	194594	1	6.687.139	5.666.046
				2,35	194595	1	7.048.918	6.372.465
					210410	2	20.158.935	18.150.022
				2,4	194596	1	4.901.760	4.519.431
					210411	2	4.881.966	4.489.679
					210239	2	3.215.927	2.999.431
				2,45	204138	1	4.696.488	4.012.696
				Above 2.45	204134	1	10.084.457	8.397.550
				Standard	194598	1	8.633.655	6.173.294
					210412	2	18.953.402	13.289.184
					210240	2	13.314.971	9.823.597
				2.35_Merged	**-**	**-**	**27.207.853**	**24.522.487**
				2.40_Merged	**-**	**-**	***12.999.653***	***12.008.541***
				Standard_Merged	**-**	**-**	**40.902.028**	**29.286.075**
				Below 2.15	194599	1	4.119.762	3.315.539
				2,2	194600	1	5.082.905	4.104.334
				2,25	194601	1	6.338.328	5.053.278
				2,3	194602	1	6.836.651	6.355.256
				2,35	194603	1	6.531.258	5.973.161
					210413	2	16.580.361	15.087.967
	Praha 5							

2338	Praha 5 - Malà Ohrada, Czech Republic	Malá Ohrada gr. 25, P7A-38770	Early Bronze Age	2,4	194604	1	7.421.646	6.631.839
					210414	2	18.405.077	16.334.281
				2,45	204135	1	4.060.547	3.213.354
				Above 2.45	204132	1	4.916.028	3.693.046
				Standard	194606	1	8.617.501	6.114.755
					210415	2	18.229.648	12.641.127
					206545	2	18.357.366	13.230.690
				2.35_Merged	**-**	**-**	***23.111.619***	***21.061.128***
				2.40_Merged	**-**	**-**	**25.826.723**	**22.966.120**
				Standard_Merged	**-**	**-**	**45.204.515**	**31.986.572**
2909	Praha 5 - Jinonice, Czech Republic	Jinonice gr. 27, P7A-16119	Iron Age	Below 2.15	194607	1	5.988.125	3.660.261
				2,2	194608	1	5.344.268	3.945.471
				2,25	194609	1	6.087.549	3.984.108
				2,3	194610	1	5.708.576	4.538.646
				2,35	194611	1	6.303.792	5.483.875
					210416	2	13.296.978	11.437.205
				2,4	194612	1	5.541.680	4.938.214
				2,45	204129	1	5.531.905	4.875.156
					210417	2	16.810.011	14.866.727
				Above 2.45	204128	1	6.719.863	5.389.570
				Standard	194614	1	6.481.420	5.046.826
					210418	2	13.748.806	10.578.619
				2.35_Merged	**-**	**-**	***19.600.770***	***16.921.080***
				2.45_Merged	**-**	**-**	**22.341.916**	**19.741.883**
				Standard_Merged	**-**	**-**	**20.230.226**	**15.625.445**
				Below 2.15	194575	1	5.329.042	3.993.431
				2,2	194576	1	7.856.551	6.048.735
				2,25	194577	1	7.147.504	5.223.275
				2,3	194578	1	8.283.251	6.466.583
				2,35	194579	1	6.618.688	5.605.328

				2,35	210419	2	18.225.701	15.241.563
2910	Praha 5 - Jinonice, Czech Republic	Jinonice gr. 35, P7A-16122	Iron Age	2,4	194580	1	5.423.607	4.769.015
					210420	2	13.643.591	11.886.762
				2,45	204133	1	11.553.250	9.598.197
				Above 2.45	204131	1	8.640.295	7.183.033
				Standard	194582	1	6.963.411	5.023.673
					210421	2	19.585.391	13.944.159
				2.35_Merged	**-**	**-**	**24.844.389**	**20.846.891**
				2.40_Merged	**-**	**-**	***19.067.198***	***16.655.777***
				Standard_Merged	**-**	**-**	**26.548.802**	**18.967.832**
P9883	Castel Sozzio, Italy	Tomb 15, Cranio V	Late Antiquity / Early Medieval	Below 2.15	194583	1	8.183.133	6.452.580
				2,2	194584	1	5.506.379	4.212.810
				2,25	194585	1	6.144.251	5.071.719
				2,3	194586	1	4.061.429	3.708.445
				2,35	194587	1	6.408.628	5.871.691
					210422	2	17.862.763	16.271.152
				2,4	194588	1	6.617.694	6.085.965
					210423	2	15.539.225	14.244.101
				2,45	204127	1	7.743.982	6.865.950
				Above 2.45	204130	1	6.948.495	6.106.369
				Standard	194590	1	6.255.053	4.768.470
					210424	2	14.920.684	11.269.277
					206546	2	10.109.523	7.769.153
				2.35_Merged	**-**	**-**	***24.271.391***	***22.142.843***
				2.40_Merged	**-**	**-**	**22.156.919**	**20.330.066**
				Standard_Merged	**-**	**-**	**31.285.260**	**23.806.900**
				Below 2.15	194631	1	6.288.876	5.031.308
				2,2	194632	1	6.047.040	4.672.501
				2,25	194633	1	6.207.466	4.842.921
				2,3	194634	1	6.473.669	5.282.051

P9884	Castel Sozzio, Italy	Tomb 27	Late Antiquity / Early Medieval	2,35	194635	1	5.886.941	5.202.313
				2,4	194636	1	6.624.378	6.117.637
					210425	2	16.885.697	15.514.676
				2,45	204147	1	8.327.546	7.383.198
					210426	2	21.723.034	19.247.495
				Above 2.45	204161	1	9.433.867	8.484.247
				Standard	194638	1	8.830.352	7.302.409
					210427	2	21.006.251	17.157.769
				2.40_Merged	**-**	**-**	**23.510.075**	**21.632.313**
				2.45_Merged	**-**	**-**	***30.050.580***	***26.630.693***
				Standard_Merged	**-**	**-**	**29.836.603**	**24.460.178**
P9892	Castel Sozzio, Italy	Tomb 19A	Late Antiquity / Early Medieval	Below 2.15	194639	1	6.742.589	4.975.392
				2,2	194640	1	5.111.485	3.630.992
				2,25	194641	1	8.627.423	8.004.415
				2,3	194642	1	6.696.418	6.271.318
				2,35	194643	1	5.755.366	5.378.243
					210428	2	18.182.243	16.936.512
				2,4	194644	1	6.435.285	6.087.076
					210429	2	16.155.507	15.245.817
				2,45	204148	1	4.717.930	4.124.221
				Above 2.45	204157	1	1.777.791	900.361
				Standard	194646	1	6.242.009	5.128.501
					210430	2	16.033.295	12.995.598
				2.35_Merged	**-**	**-**	**23.937.609**	**22.314.755**
				2.40_Merged	**-**	**-**	***22.590.792***	***21.332.893***
				Standard_Merged	**-**	**-**	**22.275.304**	**18.124.099**
				Below 2.15	194615	1	6.497.906	5.474.524
				2,2	194616	1	6.731.973	5.535.205
				2,25	194617	1	6.245.549	5.343.794
				2,3	194618	1	6.349.149	5.788.526

P9895	Castel Sozzio, Italy	Tomb 16	Late Antiquity / Early Medieval	2,35	194619	1	5.357.216	4.929.750
					210431	2	13.287.027	12.156.334
				2,4	194620	1	4.662.511	4.399.910
					210432	2	11.748.819	11.051.485
				2,45	204144	1	5.724.518	5.201.300
				Above 2.45	204159	1	5.958.729	5.575.715
				Standard	194622	1	7.049.430	6.000.388
					210433	2	15.898.447	13.402.712
				2.35_Merged	**-**	**-**	**18.644.243**	**17.086.084**
				2.40_Merged	**-**	**-**	***16.411.330***	***15.451.395***
				Standard_Merged	**-**	**-**	**22.947.877**	**19.403.100**
P9898	Castel Sozzio, Italy	Tomb 7 Ind. 1	Late Antiquity / Early Medieval	Below 2.15	194647	1	6.057.953	5.131.937
				2,2	194648	1	3.643.927	2.980.843
				2,25	194649	1	5.769.188	4.664.210
				2,3	194650	1	4.944.658	4.451.909
				2,35	194651	1	5.982.330	5.478.140
					210434	2	15.301.641	13.928.304
				2,4	194652	1	9.795.377	9.368.750
					210435	2	24.994.951	23.834.799
				2,45	204151	1	7.342.295	6.850.489
				Above 2.45	204143	1	4.915.130	4.435.627
				Standard	194654	1	7.293.275	6.844.236
					210436	2	21.248.214	19.872.834
				2.35_Merged	**-**	**-**	**21.283.971**	**19.406.444**
				2.40_Merged	**-**	**-**	***34.790.328***	***33.203.549***
				Standard_Merged	**-**	**-**	**28.541.489**	**26.717.070**
				Below 2.15	194623	1	6.734.908	5.905.663
				2,2	194624	1	6.819.145	5.587.275
				2,25	194625	1	6.865.117	5.678.012
				2,3	194626	1	7.342.559	6.379.996

P9958	Castel Sozzio, Italy	Tomb 32	Late Antiquity / Early Medieval	2,35	194627	1	6.675.307	5.852.272
					210437	2	18.066.170	15.679.369
				2,4	194628	1	6.347.061	5.830.303
					210438	2	22.905.088	20.949.758
				2,45	204150	1	9.078.398	8.374.376
				Above 2.45	204160	1	6.364.293	5.718.628
				Standard	194630	1	5.220.216	4.027.966
					210439	2	12.749.110	9.727.221
				2.35_Merged	**-**	**-**	**24.741.477**	**21.531.641**
				2.40_Merged	**-**	**-**	***29.252.149***	***26.780.061***
				Standard_Merged	**-**	**-**	**17.969.326**	**13.755.187**
Negative Controls								
SBa		-	-	-	204152	-	33.109	24.076
SBb SBb_PMD	-	-	-	-	196783	-	1.057.512	925.961
SBc	-	-	-	-	196786	-	1.259.912	1.133.708
SBd	-	-	-	-	196789	-	1.321.111	1.167.197
EBa	-	-	-	-	204139	-	807.208	544.027
EBb	-	-	-	-	196784	-	923.179	709.069
EBc	-	-	-	-	196787	-	1.091.087	937.595
EBd	-	-	-	-	196790	-	1.023.537	925.878
LBa	-	-	-	-	196788	-	1.199.514	1.071.653
LBb	-	-	-	-	196791	-	1.021.388	874.561
LBc	-	-	-	-	196782	-	830.518	664.714
LBd	-	-	-	-	196785	-	547.202	481.046
LBe	-	-	-	-	204155	-	119.685	95.332

Notes:

SB - Negative controls produced during SPT separations

EB - Negative controls produced during DNA extractions

LB - Negative controls produced during library production

All controls went through all downstream analysis treated as a normal sample

standard extraction. Filtering options and metric calculations shown below column titles. Italic merged lines denote best SPT intervals.

Aligned Reads -l 1000, -q 30, -F 4	%Endogenous (before duplicate removal) (Aligned reads / Total reads) × 100	Unique reads	%Endogenous unique (duplicates removed) (Unique reads / Total reads) × 100	%GC (unique reads)	Genomic coverage	MT coverage	Average length	Non-Normalized % Duplication rate [(Aligned reads - Unique reads) / Aligned reads] × 100
332.669	6,01	122.763	2,22	39	0.0020×	0.1764×	51	63,10
862.167	12,33	577.613	8,26	38	0.0090×	0.8164×	48	33,00
1.079.025	13,98	786.440	10,19	37	0.0134×	0.9934×	52	27,12
1.328.700	19,87	858.109	12,83	37	0.0138×	1.0764×	49	35,42
1.541.141	21,86	1.249.678	17,73	39	0.0200×	1.9255×	49	18,91
4.323.511	21,45	2.542.725	12,61	38	0.0408×	3.5181×	49	41,19
1.404.194	28,65	1.161.308	23,69	38	0.0191×	2.0930×	51	17,30
1.403.712	28,75	914.336	18,73	37	0.0152×	1.7572×	51	34,86
936.270	29,11	751.914	23,38	37	0.0124×	1.3029×	51	19,69
811.573	17,28	675.167	14,38	39	0.0097×	1.0192×	44	16,81
887.470	8,80	751.477	7,45	38	0.0109×	1.2576×	45	15,32
571.054	6,61	490.054	5,68	38	0.0083×	0.8975×	52	14,18
1.205.100	6,36	804.854	4,25	38	0.0136×	1.5103×	52	33,21
920.929	6,92	757.083	5,69	38	0.0128×	1.3531×	52	17,79
5.864.652	**21,55**	**3.565.283**	**13,10**	**38**	**0.0570×**	**4.9138×**	**49**	**39,21**
3.744.176	***28,80***	***2.698.313***	***20,76***	***37***	***0.0445×***	***4.6910×***	***51***	***27,93***
2.697.083	**6,59**	**2.032.929**	**4,97**	**38**	**0.0343×**	**3.5621×**	**52**	**24,62**
200.105	4,86	111.453	2,71	38	0.0017×	0.1954×	47	44,30
159.629	3,14	24.187	0,48	39	0.0004×	0.0340×	48	84,85
1.416.584	22,35	480.430	7,58	38	0.0076×	0.7262×	49	66,09
3.907.400	57,15	1.783.820	26,09	38	0.0305×	1.9663×	52	54,35
3.483.284	53,33	2.659.459	40,72	37	0.0444×	3.1346×	51	23,65
8.812.885	53,15	4.742.255	28,6	37	0.0791×	5.4209×	51	46,19

3.516.246	47,38	2.591.691	34,92	37	0.0424×	3.3548×	50	26,29
8.656.413	47,03	4.409.711	23,96	37	0.0720×	5.3108×	50	49,06
567.607	13,98	468.416	11,54	38	0.0072×	0.7381×	47	17,48
312.647	6,36	261.119	5,31	37	0.0040×	0.2984×	47	16,48
535.989	6,22	449.411	5,22	37	0.0078×	0.5869×	53	16,15
1.084.529	5,95	700.032	3,84	37	0.0122×	0.8754×	53	35,45
1.198.359	6,53	1.040.364	5,67	36	0.0181×	1.2801×	53	13,18
12.296.169	***53,20***	***6.595.194***	***28,54***	***37***	***0.1094×***	***7.3870×***	***51***	***46,36***
12.172.659	**47,13**	**6.047.206**	**23,41**	**37**	**0.0981×**	**7.1884×**	**50**	**50,32**
2.818.877	**6,24**	**2.183.629**	**4,83**	**37**	**0.0379×**	**2.6898×**	**53**	**22,54**
208.733	3,49	138.223	2,31	37	0.0021×	0.2415×	47	33,78
264.242	4,94	89.334	1,67	37	0.0014×	0.2079×	49	66,19
690.448	11,34	434.959	7,15	37	0.0071×	0.7645×	50	37,00
1.666.897	29,20	1.108.681	19,42	37	0.0181×	1.2747×	50	33,49
2.710.078	42,99	2.109.902	33,47	37	0.0349×	2.2818×	51	22,15
5.638.124	42,40	3.249.385	24,44	37	0.0539×	3.4202×	51	42,37
2.160.972	38,99	1.111.905	20,06	36	0.0166×	1.2724×	46	48,55
1.504.877	27,20	1.265.577	22,88	37	0.0184×	1.6350×	44	15,90
4.602.598	27,38	3.061.656	18,21	37	0.0445×	3.5697×	44	33,48
771.899	11,49	646.772	9,62	37	0.0093×	0.8918×	44	16,21
670.628	10,35	560.183	8,64	37	0.0091×	0.6711×	50	16,47
1.381.276	10,05	880.584	6,4	37	0.0143×	1.0308×	50	36,25
8.348.202	***42,59***	***4.836.166***	***24,67***	***37***	***0.0797×***	***4.9095×***	***51***	***42,07***
6.107.475	**27,34**	**4.302.730**	**19,26**	**37**	**0.0625×**	**4.9657×**	**44**	**29,55**
2.051.904	**10,14**	**1.439.090**	**7,11**	**37**	**0.0233×**	**1.6832×**	**50**	**29,87**
114.430	2,15	65.269	1,22	41	0.0011×	0.1153×	51	42,96
452.815	5,76	78.048	0,99	40	0.0012×	0.1382×	47	82,76
703.604	9,84	191.119	2,67	41	0.0031×	0.3268×	50	72,84
2.253.515	27,21	1.560.048	18,83	40	0.0266×	2.5032×	52	30,77
2.454.554	37,09	1.935.917	29,25	40	0.0333×	3.1295×	53	21,13

6.585.091	36,13	3.706.160	20,33	40	0.0640×	5.7470×	53	43,72
2.092.492	38,58	1.690.950	31,18	39	0.0287×	2.7922×	52	19,19
5.215.902	38,23	3.134.631	22,98	39	0.0535×	5.3593×	52	39,90
2.396.826	20,75	1.966.621	17,02	39	0.0307×	3.4799×	48	17,95
986.179	11,41	852.681	9,87	39	0.0128×	1.2799×	46	13,54
443.799	6,37	375.512	5,39	40	0.0068×	0.5805×	56	15,39
1.223.274	6,25	794.176	4,05	40	0.0146×	1.3071×	56	35,08
9.039.645	**36,39**	**5.304.561**	**21,35**	**40**	**0.0913×**	**8.0773×**	**53**	**41,32**
7.308.394	***38,33***	***4.596.587***	***24,11***	***39***	***0.0783×***	***7.5018×***	***52***	***37,11***
1.667.073	**6,28**	**1.167.997**	**4,40**	**40**	**0.0214×**	**1.8626×**	**56**	**29,94**
140.508	1,72	78.500	0,96	39	0.0014×	0.0971×	55	44,13
206.365	3,75	82.476	1,5	39	0.0014×	0.1030×	52	60,03
644.584	10,49	361.606	5,89	40	0.0066×	0.5662×	56	43,90
1.760.868	43,36	1.353.035	33,31	39	0.0242×	1.8607×	55	23,16
3.391.874	52,93	2.800.159	43,69	39	0.0534×	4.1016×	58	17,45
9.506.342	53,22	5.840.984	32,7	39	0.1120×	8.4569×	59	38,56
3.317.257	50,13	2.791.261	42,18	39	0.0533×	5.1900×	59	15,86
7.817.261	50,31	5.062.446	32,58	39	0.0970×	8.9742×	59	35,24
2.320.288	29,96	1.966.427	25,39	39	0.0332×	3.5283×	52	15,25
1.119.442	16,11	925.607	13,32	39	0.0149×	1.3259×	50	17,32
1.141.454	18,25	945.567	15,12	38	0.0186×	1.2677×	60	17,16
2.715.715	18,20	1.695.029	11,36	38	0.0334×	2.2394×	61	37,58
1.886.880	18,66	1.593.539	15,76	38	0.0315×	2.1768×	61	15,55
12.898.216	***53,14***	***8.478.083***	***34,93***	***39***	***0.1621×***	***11.8583×***	***59***	***34,27***
11.134.518	**50,25**	**7.787.054**	**35,15**	**39**	**0.1489×**	**13.3948×**	**59**	**30,06**
5.744.049	**18,36**	**4.226.722**	**13,51**	**38**	**0.0833×**	**5.4803×**	**61**	**26,42**
243.773	3,88	194.946	3,1	38	0.0036×	0.7060×	56	20,03
300.989	4,98	240.424	3,98	38	0.0045×	0.6460×	58	20,12
243.197	3,92	198.290	3,19	38	0.0037×	0.5689×	57	18,47
761.208	11,76	634.552	9,8	38	0.0119×	2.0170×	57	16,64

1.397.880	23,75	1.193.250	20,27	38	0.0220×	2.7954×	56	14,64
2.562.109	38,68	2.148.254	32,43	38	0.0400×	5.0559×	57	16,15
6.566.999	38,89	4.197.227	24,86	38	0.0788×	9.4137×	58	36,09
3.626.622	43,55	2.953.879	35,47	39	0.0607×	11.8927×	63	18,55
9.549.911	43,96	5.900.086	27,16	39	0.1209×	21.9333×	63	38,22
2.827.832	29,98	2.320.782	24,60	39	0.0455×	7.4463×	60	17,93
2.197.325	24,88	1.784.090	20,2	38	0.0366×	6.6072×	63	18,81
5.263.311	25,06	3.144.571	14,97	38	0.0650×	10.9781×	63	40,25
9.129.108	**38,83**	**6.315.586**	**26,86**	**38**	**0.1183×**	**13.7284×**	**57**	**30,82**
13.176.533	***43,85***	***8.833.866***	***29,40***	***39***	***0.1812×***	***30.8385×***	***63***	***32,96***
7.460.636	**25,00**	**4.922.761**	**16,50**	**38**	**0.1015×**	**16.7003×**	**63**	**34,02**
886.598	13,15	675.070	10,01	38	0.0110×	0.5821×	50	23,86
452.065	8,84	245.112	4,8	38	0.0040×	0.2413×	50	45,78
4.155.279	48,16	3.318.554	38,47	38	0.0508×	2.6910×	47	20,14
3.428.201	51,19	2.897.886	43,28	38	0.0464×	2.7750×	49	15,47
3.016.973	52,42	2.496.235	43,37	38	0.0411×	2.7834×	50	17,26
9.543.335	52,49	5.938.772	32,66	38	0.0984×	5.9551×	51	37,77
3.536.520	54,96	2.996.052	46,56	38	0.0494×	3.1401×	51	15,28
8.905.261	55,12	5.892.583	36,47	38	0.0980×	5.9868×	51	33,83
1.502.388	31,84	1.261.563	26,74	38	0.0202×	1.3697×	49	16,03
3.115	0,18	2.092	0,12	47	Below 0.0001×	0.0019×	47	32,84
1.628.675	26,09	1.389.635	22,26	37	0.0230×	1.2442×	51	14,68
4.107.434	25,62	2.718.305	16,95	37	0.0452×	2.3333×	51	33,82
12.560.308	**52,47**	**8.389.229**	**35,05**	**38**	**0.1387×**	**8.2873×**	**51**	**33,21**
12.441.781	***55,07***	***8.844.727***	***39,15***	***38***	***0.1466×***	***8.6659×***	***51***	***28,91***
5.736.109	**25,75**	**4.104.152**	**18,42**	**37**	**0.0681×**	**3.4892×**	**51**	**28,45**
1.045.823	16,09	611.868	9,42	39	0.0099×	1.3239×	49	41,49
1.282.700	19,05	400.087	5,94	38	0.0066×	0.8320×	50	68,81
846.826	13,56	546.195	8,75	40	0.0099×	1.3003×	56	35,50
2.096.679	33,02	1.719.268	27,08	39	0.0313×	3.8243×	56	18,00

2.468.462	46,08	2.087.032	38,96	39	0.0393×	4.6836×	58	15,45
6.154.447	46,32	4.014.425	30,21	39	0.0759×	8.7241×	58	34,77
2.467.777	52,93	2.112.777	45,31	38	0.0398×	5.3316×	58	14,39
6.254.977	53,24	4.140.085	35,24	38	0.0785×	10.1835×	58	33,81
1.983.723	34,65	1.653.240	28,88	39	0.0307×	3.9017×	57	16,66
1.389.543	23,32	1.156.898	19,42	38	0.0203×	2.3687×	54	16,74
1.569.566	22,27	1.323.005	18,77	38	0.0254×	2.3698×	59	15,71
3.527.404	22,19	2.264.635	14,24	38	0.0438×	4.1398×	59	35,80
8.622.909	**46,25**	**6.050.554**	**32,45**	**39**	**0.1141×**	**12.7465×**	**58**	**29,83**
8.722.754	***53,15***	***6.240.761***	***38,03***	***38***	***0.1182×***	***14.7481×***	***58***	***28,45***
5.096.970	**22,21**	**3.584.165**	**15,62**	**38**	**0.0692×**	**6.3639×**	**59**	**29,68**
1.734.565	28,63	1.197.393	19,77	39	0.0215×	2.3452×	55	30,97
988.120	27,12	650.327	17,85	38	0.0120×	1.0812×	57	34,19
1.630.551	28,26	1.122.873	19,46	39	0.0211×	1.5061×	58	31,14
2.179.544	44,08	1.742.779	35,25	39	0.0307×	2.2971×	54	20,04
3.059.903	51,15	2.545.297	42,55	39	0.0480×	4.6757×	58	16,82
7.890.819	51,57	4.953.746	32,37	39	0.0941×	8.7838×	58	37,22
5.252.572	53,62	4.301.752	43,92	40	0.0775×	9.5177×	55	18,10
13.472.803	53,90	8.124.643	32,51	40	0.1475×	17.3223×	56	39,70
3.655.089	49,78	2.955.031	40,25	38	0.0538×	7.0138×	56	19,15
1.636.624	33,30	1.352.349	27,51	39	0.0237×	2.8569×	54	17,37
2.614.160	35,84	2.181.189	29,91	41	0.0381×	3.6190×	54	16,56
7.616.575	35,85	4.819.080	22,68	41	0.0847×	7.9628×	54	36,73
10.950.722	**51,45**	**7.420.068**	**34,86**	**39**	**0.1405×**	**12.6239×**	**58**	**32,24**
18.725.375	***53,82***	***12.312.608***	***35,39***	***40***	***0.2229×***	***24.2741×***	***56***	***34,25***
10.230.735	**35,85**	**6.989.672**	**24,49**	**41**	**0.1226×**	**11.0786×**	**54**	**31,68**
2.030.726	30,15	1.683.349	24,99	39	0.0322×	3.2216×	59	17,11
1.268.160	18,60	534.636	7,84	39	0.0093×	1.1033×	53	57,84
917.060	13,36	388.276	5,66	39	0.0068×	0.6352×	54	57,66
2.612.013	35,57	1.637.023	22,29	40	0.0308×	2.9860×	58	37,33

4.010.411	60,08	3.119.491	46,73	40	0.0656×	6.0792×	65	22,22
10.974.363	60,75	6.026.772	33,36	39	0.1267×	11.1033×	65	45,08
3.740.157	58,93	3.110.199	49	39	0.0614×	6.1405×	61	16,84
13.618.385	59,46	8.494.331	37,08	39	0.1681×	15.6525×	61	37,63
5.021.365	55,31	4.101.450	45,18	39	0.0809×	8.7637×	61	18,32
1.798.080	28,25	1.502.376	23,61	39	0.0289×	2.5404×	59	16,45
1.148.851	22,01	948.583	18,17	39	0.0206×	1.5731×	67	17,43
2.813.820	22,07	1.738.362	13,64	39	0.0379×	2.8605×	67	38,22
14.984.774	**60,57**	**8.499.922**	**34,35**	**39**	**0.1774×**	**15.1916×**	**64**	**43,28**
17.358.542	***59,34***	***11.509.737***	***39,35***	***39***	***0.2275×***	***20.3115×***	***61***	***33,69***
3.962.671	**22,05**	**2.684.876**	**14,94**	**39**	**0.0584×**	**4.3720×**	**67**	**32,25**

422	1,27	328	0,99	42	Below 0.0001×	Below 0.0001×	78	22,27
21.004	1,99	9.405	0,89	46	0.0002×	0.0250×	81	55,22
		302	0,03	43	Below 0.0001×	Below 0.0001×	65	98,56
41.916	3,33	12.945	1,03	42	0.0003×	0.0489×	70	69,12
39.359	2,98	12.268	0,93	42	0.0003×	0.0421×	69	68,83
12.586	1,56	7.940	0,98	42	0.0002×	0.0206×	76	36,91
37.302	4,04	6.486	0,7	45	0.0002×	0.0048×	79	82,61
19.741	1,81	4.583	0,42	43	0.0001×	0.0106×	68	76,78
11.159	1,09	7.078	0,69	42	0.0002×	0.0030×	67	36,57
10.374	0,86	3.687	0,31	42	0.0001×	0.0089×	66	64,46
24.400	2,39	4.377	0,43	42	0.0001×	0.0036×	65	82,06
8.170	0,98	1.406	0,17	42	Below 0.0001×	Below 0.0001×	45	82,79
7.327	1,34	1.906	0,35	40	Below 0.0001×	Below 0.0001×	69	73,99
110	0,09	26	0,02	48	Below 0.0001×	Below 0.0001×	43	76,36

Contamination % via hapCon from Huang & Ringbauer (2023) **(95% CI) - Number of used SNPs**	**Deamination Frequency 5'**	**Deamination Frequency 3'**	**Molecular Sex Assignment via ry_compute from Skoglund et al. (2013)**
N/A (too few data)	0,35	0,35	XY
12.79 (2.44 - 23.14) - 870	0,42	0,41	XY
2.20 (-2.05 - 6.45) - 1313	0,38	0,37	XY
4.88 (0.10 - 9.66) - 1344	0,41	0,39	XY
1.60 (-0.91 - 4.12) - 1954	0,42	0,40	XY
4.86 (2.89 - 6.82) - 4007	0,42	0,40	XY
4.26 (1.04 - 7.49) - 1871	0,44	0,41	XY
2.60 (-1.59 - 6.78) - 1442	0,44	0,42	XY
4.06 (-1.19 - 9.31) - 1180	0,44	0,41	XY
2.76 (-4.91 - 10.43) - 907	0,38	0,37	XY
2.95 (-3.01 - 8.91) - 1024	0,36	0,35	XY
N/A (too few data)	0,40	0,38	XY
7.65 (1.06 - 14.24) - 134	0,40	0,38	XY
4.36 (-1.09 - 9.82) - 1230	0,40	0,38	XY
3.70 (2.17 - 5.24) - 5535	**0,42**	**0,40**	**XY**
2.81 (1.14 - 4.48) - 4264	***0,44***	***0,41***	***XY***
4.79 (2.42 - 7.16) - 3318	**0,40**	**0,38**	**XY**
N/A (too few data)	0,33	0,32	Consistent with XY but not XX
N/A (too few data)	0,29	0,28	Consistent with XY but not XX
0.00 (-7.86 - 7.86) - 755	0,33	0,32	Consistent with XY but not XX
1.68 (0.03 - 3.32) - 3013	0,35	0,34	XY
1.83 (0.32 - 3.35) - 4349	0,36	0,34	XY
2.30 (1.31 - 3.29) - 7744	0,36	0,34	XY

3.20 (1.64 - 4.76) - 4198	0,36	0,35	XY
2.70 (1.57 - 3.83) - 7095	0,36	0,35	XY
0.00 (-6.92 - 6.92) - 651	0,33	0,31	XY
N/A (too few data)	0,33	0,32	XY
0.00 (-5.88 - 5.88) - 776	0,35	0,33	XY
3.27 (-0.44 - 6.98) - 1183	0,35	0,33	XY
0.18 (-2.38 - 2.73) - 1747	0,35	0,33	XY
2.82 (1.93 - 3.70) - 10577	***0,36***	***0,34***	***XY***
2.68 (1.75 - 3.61) - 9610	**0,36**	**0,35**	**XY**
2.11 (0.44 - 3.77) - 3661	**0,35**	**0,33**	**XY**
50.00 (-36.74 - 136.74) - 226	0,37	0,37	Consistent with XY but not XX
N/A (too few data)	0,38	0,38	Consistent with XY but not XX
10.99 (-0.69 - 22.68) - 735	0,38	0,37	XY
0.00 (-1.92 - 1.92) - 1782	0,38	0,38	XY
3.58 (1.36 - 5.81) - 3362	0,41	0,40	XY
1.76 (0.57 - 2.96) - 5214	0,41	0,40	XY
2.63 (-0.64 - 5.91) - 1604	0,34	0,30	XY
3.70 (0.54 - 6.87) - 1843	0,35	0,35	XY
3.50 (1.85 - 5.14) - 4225	0,36	0,35	XY
3.77 (-5.04 - 12.57) - 868	0,36	0,35	XY
4.94 (-3.34 - 13.23) - 863	0,37	0,37	XY
3.86 (-0.81 - 8.52) - 1398	0,37	0,37	XY
2.79 (1.68 - 3.91) - 7602	***0,41***	***0,41***	***XY***
3.55 (2.22 - 4.88) - 5989	**0,35**	**0,35**	**XY**
2.69 (-0.03 - 5.40) - 2256	**0,37**	**0,37**	**XY**
7.68 (-0.32 - 15.68) - 661	0,28	0,26	XY
N/A (too few data)	0,32	0,31	Consistent with XY but not XX
50.00 (-12.06 - 112.06) - 275	0,30	0,29	XY
2.61 (0.55 - 4.66) - 2499	0,31	0,29	XY
2.07 (0.27 - 3.88) - 3164	0,31	0,29	XY

3.40 (2.08 - 4.71) - 6142	0,31	0,29	XY
3.07 (0.88 - 5.26) - 2679	0,32	0,30	XY
1.48 (0.27 - 2.68) - 5116	0,32	0,30	XY
2.34 (0.23 - 4.44) - 2838	0,29	0,29	XY
7.37 (1.71 - 13.03) - 1156	0,28	0,28	XY
N/A (too few data)	0,29	0,27	XY
2.14 (-1.23 - 5.51) - 1445	0,29	0,27	XY
2.88 (1.88 - 3.87) - 8655	**0,31**	**0,29**	**XY**
1.72 (0.75 - 2.68) - 7383	***0,32***	***0,30***	***XY***
2.00 (-0.47 - 4.47) - 2099	**0,29**	**0,27**	**XY**
N/A (too few data)	0,27	0,26	Consistent with XY but not XX
N/A (too few data)	0,27	0,26	Consistent with XY but not XX
9.59 (-2.16 - 21.34) - 616	0,32	0,31	XY
1.66 (-0.90 - 4.23) - 2319	0,36	0,35	XY
2.70 (1.23 - 4.17) - 5131	0,32	0,29	XY
2.78 (1.88 - 3.67) - 10681	0,32	0,30	XY
3.69 (2.16 - 5.23) - 5090	0,35	0,32	XY
2.72 (1.75 - 3.70) - 9241	0,35	0,33	XY
2.76 (0.79 - 4.73) - 3258	0,32	0,30	XY
0.70 (-2.75 - 4.16) - 1432	0,28	0,24	XY
0.20 (-1.52 - 1.93) - 1877	0,31	0,28	XY
0.86 (-0.49 - 2.22) - 3344	0,31	0,28	XY
0.70 (-0.89 - 2.29) - 3046	0,31	0,28	XY
2.76 (2.05 - 3.46) - 15218	***0,32***	***0,30***	***XY***
3.09 (2.32 - 3.86) - 13978	**0,35**	**0,33**	**XY**
1.30 (0.44 - 2.15) - 8115	**0,31**	**0,28**	**XY**
N/A (too few data)	0,29	0,26	XY
N/A (too few data)	0,29	0,27	XY
19.23 (-16.07 - 54.53) - 396	0,29	0,26	Consistent with XY but not XX
16.91 (8.00 - 25.82) - 1125	0,31	0,28	XY

4.48 (1.35 - 7.60) - 2174	0,31	0,29	XY
3.67 (1.75 - 5.59) - 3948	0,31	0,28	XY
3.40 (2.22 - 4.59) - 7627	0,31	0,28	XY
3.37 (1.99 - 4.76) - 5958	0,31	0,27	XY
3.88 (2.91 - 4.85) - 11708	0,31	0,27	XY
2.14 (0.64 - 3.65) - 4563	0,33	0,29	XY
3.17 (1.16 - 5.17) - 3609	0,31	0,27	XY
2.37 (1.09 - 3.65) - 6398	0,31	0,27	XY
3.60 (2.64 - 4.55) - 11335	**0,31**	**0,28**	**XY**
4.09 (3.32 - 4.86) - 17235	***0,31***	***0,27***	***XY***
2.51 (1.55 - 3.47) - 9869	**0,31**	**0,27**	**XY**
1.01 (-4.39 - 6.40) - 1065	0,29	0,26	XY
41.80 (3.45 - 80.15) - 425	0,28	0,26	Consistent with XY but not XX
2.02 (0.61 - 3.42) - 4761	0,30	0,29	XY
2.16 (0.66 - 3.67) - 4294	0,30	0,29	XY
1.89 (0.32 - 3.45) - 3853	0,30	0,29	XY
2.39 (1.47 - 3.31) - 9230	0,30	0,29	XY
2.35 (0.84 - 3.85) - 4567	0,31	0,30	XY
3.02 (2.03 - 4.01) - 9245	0,31	0,30	XY
1.37 (-1.21 - 3.94) - 1962	0,29	0,29	XY
N/A (too few data)	0,14	0,13	Not Assigned
2.49 (-0.40 - 5.38) - 2109	0,29	0,28	XY
2.65 (1.01 - 4.30) - 4274	0,29	0,28	XY
2.60 (1.83 - 3.37) - 12775	**0,30**	**0,29**	**XY**
2.75 (2.00 - 3.51) - 13495	***0,31***	***0,30***	***XY***
2.62 (1.41 - 3.82) - 6512	**0,29**	**0,28**	**XY**
N/A (female)	0,33	0,32	XX
N/A (female)	0,33	0,32	XX
N/A (female)	0,27	0,26	XX
N/A (female)	0,32	0,30	XX

N/A (female)	0,31	0,29	XX
N/A (female)	0,31	0,29	XX
N/A (female)	0,33	0,32	XX
N/A (female)	0,34	0,31	XX
N/A (female)	0,32	0,30	XX
N/A (female)	0,35	0,32	XX
N/A (female)	0,31	0,29	XX
N/A (female)	0,31	0,29	XX
N/A (female)	**0,31**	**0,29**	**XX**
N/A (female)	***0,34***	***0,32***	***XX***
N/A (female)	**0,31**	**0,29**	**XX**
9.92 (5.77 - 14.07) - 2097	0,29	0,28	XY
8.20 (2.14 - 14.25) - 1287	0,28	0,26	XY
2.42 (-0.27 - 5.11) - 2072	0,27	0,25	XY
3.09 (1.09 - 5.09) - 2860	0,27	0,26	XY
2.96 (1.34 - 4.58) - 4613	0,29	0,26	XY
1.46 (0.66 - 2.25) - 8960	0,29	0,26	XY
2.48 (1.41 - 3.56) - 7386	0,32	0,30	XY
2.00 (1.34 - 2.65) - 13677	0,32	0,30	XY
2.95 (1.58 - 4.32) - 5323	0,31	0,30	XY
3.83 (0.92 - 6.75) - 2320	0,31	0,29	XY
2.38 (0.88 - 3.88) - 3617	0,27	0,26	XY
2.13 (1.20 - 3.07) - 8096	0,27	0,26	XY
1.91 (1.23 - 2.59) - 13235	**0,29**	**0,26**	**XY**
2.32 (1.78 - 2.85) - 20254	***0,32***	***0,30***	***XY***
2.36 (1.59 - 3.12) - 11523	**0,27**	**0,26**	**XY**
N/A (female)	0,31	0,28	XX
N/A (female)	0,29	0,27	XX
N/A (female)	0,29	0,28	XX
N/A (female)	0,30	0,28	XX

N/A (female)	0,29	0,24	XX
N/A (female)	0,29	0,25	XX
N/A (female)	0,31	0,28	XX
N/A (female)	0,31	0,28	XX
N/A (female)	0,31	0,28	XX
N/A (female)	0,31	0,28	XX
N/A (female)	0,28	0,24	XX
N/A (female)	0,28	0,24	XX
N/A (female)	**0,29**	**0,25**	**XX**
N/A (female)	***0,31***	***0,28***	***XX***
N/A (female)	**0,28**	**0,24**	**XX**

-	0,00	0,00	Inconclusive
-	0,02	0,02	Consistent with XX but not XY
	0,70	0,55	Consistent with XX
-	0,00	0,00	Consistent with XX but not XY
-	0,00	0,00	Not Assigned
-	0,00	0,00	Consistent with XX but not XY
-	0,00	0,00	Not Assigned
-	0,00	0,00	Consistent with XY but not XX
-	0,00	0,00	Consistent with XY but not XX
-	0,00	0,00	Consistent with XX but not XY
-	0,00	0,00	Consistent with XX but not XY
-	0,00	0,00	Inconclusive
-	0,00	0,00	Not Assigned
-	0,00	0,00	Inconclusive

Ry_compute output from Skoglund et al. (2013)

(number of ChrY reads / total ChrX+ChrY reads)

Ry=0.0894 with 95% CI:0.0799-0.0989 (ChrY:310/3467)
Ry=0.08465 with 95% CI:0.0803-0.089 (ChrY:1350/15951)
Ry=0.08805 with 95% CI:0.0843-0.0918 (ChrY:1921/21810)
Ry=0.0846 with 95% CI:0.0811-0.0881 (ChrY:2074/24516)
Ry=0.085 with 95% CI:0.0821-0.0879 (ChrY:2985/35108)
Ry=0.0866 with 95% CI:0.0845-0.0887 (ChrY:6186/71423)
Ry=0.08655 with 95% CI:0.0835-0.0896 (ChrY:2852/32960)
Ry=0.0876 with 95% CI:0.0841-0.0911 (ChrY:2250/25683)
Ry=0.08815 with 95% CI:0.0843-0.092 (ChrY:1863/21131)
Ry=0.0833 with 95% CI:0.0793-0.0873 (ChrY:1535/18435)
Ry=0.0853 with 95% CI:0.0815-0.0891 (ChrY:1769/20736)
Ry=0.08835 with 95% CI:0.0836-0.0931 (ChrY:1221/13820)
Ry=0.0832 with 95% CI:0.0796-0.0868 (ChrY:1876/22544)
Ry=0.08715 with 95% CI:0.0834-0.0909 (ChrY:1852/21252)
Ry=0.08615 with 95% CI:0.0844-0.0879 (ChrY:8630/100164)
Ry=0.0869 with 95% CI:0.0849-0.0889 (ChrY:6617/76162)
Ry=0.0858 with 95% CI:0.0835-0.0881 (ChrY:4902/57125)
Ry=0.4007 with 95% CI:0.0711-0.0904 (ChrY:249/3083)
Ry=0.06785 with 95% CI:0.0489-0.0868 (ChrY:46/678)
Ry=0.07945 with 95% CI:0.0749-0.084 (ChrY:1069/13457)
Ry=0.0835 with 95% CI:0.0811-0.0859 (ChrY:4185/50128)
Ry=0.08385 with 95% CI:0.0819-0.0858 (ChrY:6336/75556)
Ry=0.0842 with 95% CI:0.0827-0.0857 (ChrY:11264/133833)

Ry=0.0838 with 95% CI:0.0818-0.0858 (ChrY:6205/74024)

Ry=0.08485 with 95% CI:0.0833-0.0864 (ChrY:10723/126390)

Ry=0.0806 with 95% CI:0.0759-0.0853 (ChrY:1030/12779)

Ry=0.08185 with 95% CI:0.0756-0.0881 (ChrY:602/7354)

Ry=0.0813 with 95% CI:0.0766-0.086 (ChrY:1038/12768)

Ry=0.08425 with 95% CI:0.0804-0.0881 (ChrY:1676/19885)

Ry=0.08445 with 95% CI:0.0813-0.0876 (ChrY:2513/29770)

Ry=0.08375 with 95% CI:0.0825-0.085 (ChrY:15620/186460)

Ry=0.0842 with 95% CI:0.0829-0.0855 (ChrY:14561/172907)

Ry=0.08375 with 95% CI:0.0816-0.0859 (ChrY:5215/62281)

Ry=0.0817 with 95% CI:0.073-0.0904 (ChrY:310/3793)

Ry=0.08435 with 95% CI:0.0736-0.0951 (ChrY:216/2560)

Ry=0.0846 with 95% CI:0.0797-0.0895 (ChrY:1049/12405)

Ry=0.08495 with 95% CI:0.0819-0.088 (ChrY:2697/31745)

Ry=0.08455 with 95% CI:0.0823-0.0868 (ChrY:5046/59666)

Ry=0.0876 with 95% CI:0.0858-0.0894 (ChrY:8102/92470)

Ry=0.0822 with 95% CI:0.0792-0.0852 (ChrY:2578/31365)

Ry=0.08465 with 95% CI:0.0817-0.0876 (ChrY:2965/35026)

Ry=0.08285 with 95% CI:0.081-0.0847 (ChrY:6987/84344)

Ry=0.08375 with 95% CI:0.0797-0.0878 (ChrY:1492/17814)

Ry=0.0866 with 95% CI:0.0822-0.091 (ChrY:1350/15594)

Ry=0.08755 with 95% CI:0.084-0.0911 (ChrY:2147/24531)

Ry=0.08395 with 95% CI:0.0845-0.0874 (ChrY:11804/137325)

Ry=0.08325 with 95% CI:0.0817-0.0848 (ChrY:9880/118693)

Ry=0.08705 with 95% CI:0.0843-0.0898 (ChrY:3490/40092)

Ry=0.0896 with 95% CI:0.0761-0.1031 (ChrY:154/1718)

Ry=0.086 with 95% CI:0.0743-0.0977 (ChrY:190/2210)

Ry=0.09125 with 95% CI:0.0834-0.0991 (ChrY:470/5150)

Ry=0.0888 with 95% CI:0.0861-0.0915 (ChrY:3763/42389)

Ry=0.0868 with 95% CI:0.0844-0.0892 (ChrY:4596/52936)

Ry=0.0866 with 95% CI:0.0849-0.0883 (ChrY:8832/102006)

Ry=0.0884 with 95% CI:0.0858-0.091 (ChrY:4127/46674)

Ry=0.0872 with 95% CI:0.0853-0.0891 (ChrY:7516/86199)

Ry=0.08555 with 95% CI:0.0832-0.0879 (ChrY:4644/54272)

Ry=0.0835 with 95% CI:0.0799-0.0871 (ChrY:1931/23125)

Ry=0.09215 with 95% CI:0.0866-0.0977 (ChrY:958/10392)

Ry=0.0888 with 95% CI:0.085-0.0926 (ChrY:1951/21971)

Ry=0.0865 with 95% CI:0.0851-0.0879 (ChrY:12598/145635)

Ry=0.08745 with 95% CI:0.0859-0.089 (ChrY:11064/126578)

Ry=0.0899 with 95% CI:0.0868-0.093 (ChrY:2905/32318)

Ry=0.082 with 95% CI:0.0706-0.0934 (ChrY:182/2219)

Ry=0.0843 with 95% CI:0.0732-0.0954 (ChrY:203/2408)

Ry=0.08785 with 95% CI:0.0823-0.0934 (ChrY:879/10006)

Ry=0.08535 with 95% CI:0.0825-0.0882 (ChrY:3163/37066)

Ry=0.0882 with 95% CI:0.0862-0.0902 (ChrY:6874/77932)

Ry=0.08675 with 95% CI:0.0854-0.0881 (ChrY:14178/163444)

Ry=0.0888 with 95% CI:0.0868-0.0908 (ChrY:6898/77692)

Ry=0.08625 with 95% CI:0.0848-0.0877 (ChrY:12151/140919)

Ry=0.08435 with 95% CI: 0.082-0.0867 (ChrY:4550/53926)

Ry=0.08715 with 95% CI:0.0837-0.0906 (ChrY:2233/25616)

Ry=0.0876 with 95% CI:0.0842-0.091 (ChrY:2329/26583)

Ry=0.0895 with 95% CI:0.0869-0.0921 (ChrY:4230/47259)

Ry=0.08585 with 95% CI:0.0833-0.0884 (ChrY:3868/45059)

Ry=0.08695 with 95% CI:0.0858-0.0881 (ChrY:20608/236926)

Ry=0.087 with 95% CI:0.0858-0.0882 (ChrY:18868/216875)

Ry=0.0877 with 95% CI:0.0861-0.0893 (ChrY:10413/118781)

Ry=0.0874 with 95% CI:0.08-0.0948 (ChrY:490/5606)

Ry=0.08735 with 95% CI:0.0806-0.0941 (ChrY:588/6731)

Ry=0.0803 with 95% CI:0.0733-0.0873 (ChrY:464/5776)

Ry=0.08845 with 95% CI:0.0843-0.0926 (ChrY:1603/18117)

Ry=0.0854 with 95% CI:0.0824-0.0884 (ChrY:2883/33764)
Ry=0.0854 with 95% CI:0.0832-0.0876 (ChrY:5199/60885)
Ry=0.0876 with 95% CI:0.086-0.0892 (ChrY:10462/119411)
Ry=0.09005 with 95% CI:0.0881-0.092 (ChrY:7530/83625)
Ry=0.08945 with 95% CI:0.0881-0.0908 (ChrY:14994/167658)
Ry=0.0892 with 95% CI:0.087-0.0914 (ChrY:5889/66005)
Ry=0.08705 with 95% CI:0.0846-0.0895 (ChrY:4431/50891)
Ry=0.08865 with 95% CI:0.0868-0.0905 (ChrY:7988/90073)
Ry=0.0868 with 95% CI:0.0855-0.0881 (ChrY:15582/179524)
Ry=0.0896 with 95% CI:0.0885-0.0907 (ChrY:22470/250823)
Ry=0.08805 with 95% CI:0.0866-0.0895 (ChrY:12401/140845)
Ry=0.08125 with 95% CI:0.0774-0.0851 (ChrY:1541/18967)
Ry=0.0805 with 95% CI:0.074-0.087 (ChrY:540/6709)
Ry=0.0819 with 95% CI:0.0801-0.0837 (ChrY:7422/90654)
Ry=0.08305 with 95% CI:0.0811-0.085 (ChrY:6586/79298)
Ry=0.0839 with 95% CI:0.0818-0.086 (ChrY:5732/68322)
Ry=0.08295 with 95% CI:0.0816-0.0843 (ChrY:13618/164130)
Ry=0.08395 with 95% CI:0.0821-0.0858 (ChrY:6951/82793)
Ry=0.08475 with 95% CI:0.0834-0.0861 (ChrY:13885/163764)
Ry=0.0851 with 95% CI:0.0822-0.088 (ChrY:2981/35027)
Ry=0.03845 with 95% CI:-0.0138-0.0907 (ChrY:2/52)
Ry=0.08505 with 95% CI:0.0823-0.0878 (ChrY:3274/38500)
Ry=0.0832 with 95% CI:0.0812-0.0852 (ChrY:6257/75222)
Ry=0.08315 with 95% CI:0.082-0.0843 (ChrY:19228/231265)
Ry=0.0844 with 95% CI:0.0833-0.0855 (ChrY:20717/245495)
Ry=0.0837 with 95% CI:0.0821-0.0853 (ChrY:9511/113642)
Ry=0.0047 with 95% CI:0.0039-0.0055 (ChrY:143/30422)
Ry=0.0043 with 95% CI:0.0034-0.0052 (ChrY:85/19911)
Ry=0.0049 with 95% CI:0.0041-0.0057 (ChrY:130/26552)
Ry=0.004 with 95% CI:0.0036-0.0044 (ChrY:343/85269)

Ry=0.00375 with 95% CI:0.0034-0.0041 (ChrY:390/103808)

Ry=0.00375 with 95% CI:0.0035-0.004 (ChrY:757/200936)

Ry=0.00365 with 95% CI:0.0033-0.004 (ChrY:387/106702)

Ry=0.00365 with 95% CI:0.0034-0.0039 (ChrY:756/208959)

Ry=0.0038 with 95% CI:0.0034-0.0042 (ChrY:316/83018)

Ry=0.0038 with 95% CI:0.0033-0.0043 (ChrY:221/58723)

Ry=0.0037 with 95% CI:0.0032-0.0042 (ChrY:245/66055)

Ry=0.00385 with 95% CI:0.0035-0.0042 (ChrY:438/113899)

Ry=0.00375 with 95% CI:0.0035-0.004 (ChrY:1131/302317)

Ry=0.0036 with 95% CI:0.0034-0.0038 (ChrY:1135/315115)

Ry=0.0038 with 95% CI:0.0035-0.0041 (ChrY:679/179834)

Ry=0.08455 with 95% CI:0.0816-0.0875 (ChrY:2864/33880)

Ry=0.08085 with 95% CI:0.0769-0.0848 (ChrY:1493/18461)

Ry=0.085 with 95% CI:0.0819-0.0881 (ChrY:2667/31379)

Ry=0.08115 with 95% CI:0.0787-0.0836 (ChrY:3867/47669)

Ry=0.08625 with 95% CI:0.0842-0.0883 (ChrY:6084/70528)

Ry=0.0874 with 95% CI:0.0859-0.0889 (ChrY:12031/137645)

Ry=0.08465 with 95% CI:0.0831-0.0862 (ChrY:10047/118676)

Ry=0.08485 with 95% CI:0.0837-0.086 (ChrY:19090/224900)

Ry=0.086 with 95% CI:0.0841-0.0879 (ChrY:7242/84214)

Ry=0.088 with 95% CI:0.0851-0.0909 (ChrY:3282/37293)

Ry=0.08675 with 95% CI:0.0845-0.089 (ChrY:5216/60103)

Ry=0.08785 with 95% CI:0.0863-0.0894 (ChrY:11652/132614)

Ry=0.0869 with 95% CI:0.0857-0.0881 (ChrY:17903/206075)

Ry=0.0847 with 95% CI:0.0838-0.0856 (ChrY:28859/340687)

Ry=0.08735 with 95% CI:0.0861-0.0886 (ChrY:16821/192518)

Ry=0.0042 with 95% CI:0.0038-0.0046 (ChrY:353/83968)

Ry=0.00495 with 95% CI:0.0041-0.0058 (ChrY:130/26441)

Ry=0.00665 with 95% CI:0.0055-0.0078 (ChrY:128/19323)

Ry=0.00425 with 95% CI:0.0038-0.0047 (ChrY:344/81247)

Ry=0.00455 with 95% CI:0.0042-0.0049 (ChrY:707/154592)

Ry=0.0041 with 95% CI:0.0039-0.0043 (ChrY:1234/300157)

Ry=0.0042 with 95% CI:0.0039-0.0045 (ChrY:647/154324)

Ry=0.0041 with 95% CI:0.0039-0.0043 (ChrY:1754/423420)

Ry=0.0044 with 95% CI:0.0041-0.0047 (ChrY:906/204553)

Ry=0.00445 with 95% CI:0.004-0.0049 (ChrY:340/75977)

Ry=0.0046 with 95% CI:0.004-0.0052 (ChrY:216/47302)

Ry=0.0039 with 95% CI:0.0035-0.0043 (ChrY:338/87252)

Ry=0.0043 with 95% CI:0.0041-0.0045 (ChrY:1802/423153)

Ry=0.00415 with 95% CI:0.004-0.0043 (ChrY:2365/573261)

Ry=0.00415 with 95% CI:0.0038-0.0045 (ChrY:553/134491)

Ry=0 with 95% CI:0.0-0.0, but consistent with XX (ChrY:0/13)

Ry=0.02675 with 95% CI:0.0104-0.0431 (ChrY:10/374)

Ry=0 with 95% CI:0.0-0.0, but consistent with XX (ChrY:0/16)

Ry=0.02125 with 95% CI:0.0088-0.0337 (ChrY:11/517)

Ry=0.0387 with 95% CI:0.0216-0.0558 (ChrY:19/491)

Ry=0.0156 with 95% CI:0.002-0.0292 (ChrY:5/320)

Ry=0.04545 with 95% CI:0.0164-0.0745 (ChrY:9/198)

Ry=0.0699 with 95% CI:0.0333-0.1065 (ChrY:13/186)

Ry=0.0652 with 95% CI:0.0333-0.0971 (ChrY:15/230)

Ry=0.02225 with 95% CI:-0.0026-0.0471 (ChrY:3/135)

Ry=0.02825 with 95% CI:0.0038-0.0527 (ChrY:5/177)

Ry=0 with 95% CI:0.0-0.0, but consistent with XX (ChrY:0/43)

Ry=0.0435 with 95% CI:-0.0046-0.0916 (ChrY:3/69)

Ry=0 with 95% CI:0.0-0.0, but consistent with XX (ChrY:0/1)